ULTRA-SMALL MODULAR REACTOR: ECONOMIC AND DESIGN ANALYSIS

A Thesis
Presented to
The Academic Faculty

By

Naiki A. Kaffezakis

In Partial Fulfillment
of the Requirements for the Degree
Masters of Science in
Nuclear and Radiological Engineering

Georgia Institute of Technology

December 2019

ULTRA-SMALL MODULAR REACTOR: ECONOMIC AND DESIGN ANALYSIS

Approved by:

Dr. Dan Kotlyar
School of Mechanical Engineering
Georgia Institute of Technology

Dr. Bojan Petrovic
School of Mechanical Engineering
Georgia Institute of Technology

Dr. Anna Erickson
School of Mechanical Engineering
Georgia Institute of Technology

Date Approved: November 14, 2019

I dedicate this work to Scout Schultz, Dallas Punja, and Kirby Jackson. May they rest in power and never be forgotten.

ACKNOWLEDGEMENTS

First, I would like to acknowledge my adviser Dr. Dan Kotlyar. His willingness to take the risk in assigning my own project to lead as an undergraduate has been monumental in developing my interests in research and academia. On top of providing technical guidance, Dr. Kotlyar has shown me great moral support in an, at times, truly harrowing past couple of years. His belief in my capabilities has often outweighed my own confidence, and I have truly appreciated his invitation to join his lab as a graduate student and to manage the USMR project. For all this and more, Dr. Kotlyar has my utmost gratitude.

Second, I would like to provide praise for my colleagues who have helped in the development of the work. For his aide in putting together the material parameters database used in this computational analysis, I would like to thank Stefano Terlizzi. I would also like to acknowledge Corey Smith, Andrew Neslon, and Ian Miner who I have had the privilege to mentor while as undergraduates and who have provided significant aide in running and collecting results from the computational models.

Next, in putting together the concept and interdisciplinary team for the USMR project, I would like to acknowledge Dr. Shannon Yee. I would alos like to express gratitude to Dr. Seyf Hamidreza, Dr. Upadhyaya Ajay, Dr. Rohatgi Ajeet, and Dr. Henry Asegun for providing and sharing their knowledge and experience with TPV cells.

Lastly I would like to share my undying love for my friends, family, partner, and community who have been endlessly patient and fabulously supportive while I have pursued these endeavors.

TABLE OF CONTENTS

LIST OF TABLES

LIST OF FIGURES

SUMMARY

This thesis presents the pre-conceptual computational and economic analysis of a high-temperature (>1300 K), ultra-small (<10 MWe) modular reactor with a coupled high-efficiency (>50%) thermophotovoltaic (TPV) power block. Inspired by decreasing costs in TPV manufacturing, the integration of the TPV power block would allow for improved electrification efficiency over the heat cycles of traditional nuclear power plants. Further, by not requiring a pressure vessel and coolant loops, a USMR powered plant could feature significantly lower capital costs and be would be impervious to many of the major accident scenarios of typical plants. However, allowing for heat removal solely through radiative and passive convective cooling puts steep limitations on the USMR operational power densities and the selection of materials. This thesis reports on three phases of the USMR study: an initial sampling of the design space, a comprehensive economic analysis, and a focused study on improving fuel utilization. The preliminary sampling of the design space was performed using coupled thermal and neutronic analysis on a simplified model and resulted in the decision to focus on uranium carbide and uranium nitride fuels as the most promising fuel candidates. A top-down differential economic analysis, utilizing the Gen IV International Forum cost estimation guidelines and the Energy Economic Database, showed that USMR could potentially outperform larger plants in levelized cost of electricity, an extraordinary feat for a microreactor. An examination of power scaling factors and learning curves was also undertaken and suggests that there is a route for multi-unit siting to overcome loss of economies of scale for the USMR. The economic analysis highlighted fuel utilization as a major factor in USMR cost which led to a more focused exploration of the USMR design space, examining the tradeoff between maximum power density and fuel utilization while varying the moderation ratio of the core. This led to a converged design that could potentially produce electricity with a levelized cost as low as $39 per MWhr, as compared to the $93 per MWhr cost of the typical generation III+ nuclear plant.

CHAPTER 1
INTRODUCTION AND BACKGROUND

1.1 Introduction and Outline

This thesis covers the development of the Ultra Small Modular Reactor (USMR) concept, a micro-modular reactor design under development by an inter-disciplinary team at Georgia Institute of Technology, involving experts in reactor physics, energy systems, and photovoltaics [1]. The USMR design is ground breaking in that it eschews the standard model of using a Rankine (or Brayton) cycle to cool the core and generate electricity. In the USMR design, electricity is produced by coupling a small reactor core, wrapped in a tungsten photon emitter with thermophotovoltaic (TPV) cells. By operating the core at high temperatures, greater than 1300 K, at the outer boundary, electricity production efficiencies of well over 50% are possible using modern TPV technology. Furthermore, the USMR reactor is operated at relatively low power densities ($< 2W/cm^3$), allowing the design to be cooled via natural convection and leads to cycle lengths of several decades.

Following an introduction and conceptual background presented here in Chapter 1, this work covers the initial exploration of the design space through a custom built framework for coupled neutronic and thermal computational analysis. The construction of this framework is laid out in Chapter 2 and the results of the initial exploration are presented in Chapter 3. The initial examination of the USMR design was followed up by the development of economic models to provide estimates for construction and operational costs and evaluate economic viability. Chapter 4 presents the economic model and analysis in depth and present the key design recommendations that were born from the analysis. Informed by the economic tools, a second design space analysis was undertaken to develop an economically ideal USMR design, which is outlined in Chapter 5. Lastly, Chapter 6 presents the final

conclusions from this extensive techno-economic analysis as well as ongoing and future work on the USMR project.

1.2 Current State of Nuclear Systems

The promise of the nuclear renaissance of the early 2000s, once lauded as the the key to reviving this sleeping giant in the carbon free energy enterprise has turned to despair in the USA and Europe. Though often blamed on the turn of public opinion following the Fukushima accident, the end of the dream has more to do with economics. The generation 3 advanced designs with their inherent safety features and modular construction have not been able to overcome the weaknesses in the western nuclear industry. In the United States, half of the new Westinghouse AP1000 reactors that were ordered have been abandoned and the other two being constructed at Plant Vogtle in Georgia have been plagued with cost overruns and construction delays. Similar scenarios are playing out in the UK, Finland and France. Meanwhile, China has brought 8 new reactors online in the past year and is on schedule to complete 10 more a year starting in 2020 [2]. In the Middle East, Russia and South Korea new plants have been completed without a hitch. On average, the East has been able to produce new reactors at a third of the cost and in half the time.

It is trivial to point to decreased labor costs in these eastern countries as part of their success. However, as can be seen in the Figure 1.1 below, the cost of recent construction in the west, specifically in the UK, has exceeded the estimates drawn from the energy economic database (EEDB) and greatly overrun targets for economic competitiveness in every category [2]. Based on the collective final cost breakdowns of nuclear plants constructed in the United States during the first nuclear construction boom in the 1970s and 1980s, the EEDB has become a standard for nuclear economic analysis [3]. Figure 1.1 brings into question the validity of applying this data set to current and future projects. However, it is significant to note that the categorical breakdown of the estimates into overnight (Materials, Policy, and Vendor Equipment) and time dependent costs (Project Design, Construction Excel-

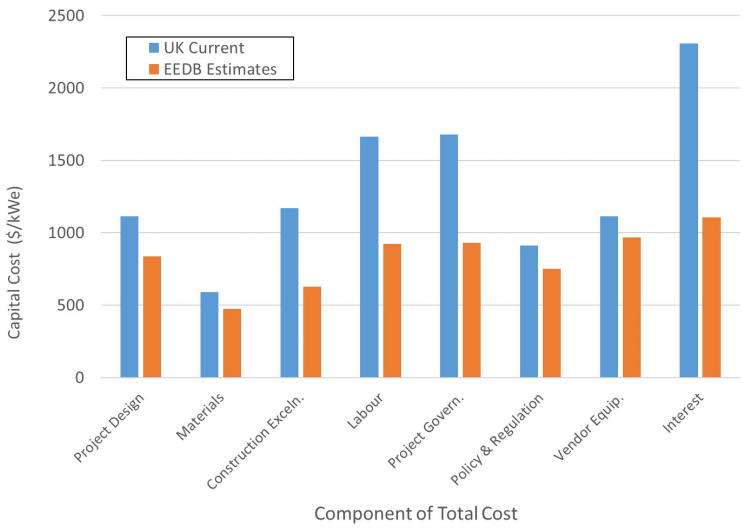

Figure 1.1. Current costs of reactors built in the UK as compared to target costs and estimates based on the EEDB, adapted from Roulstone, 2019 [2].

lence, Labor, Project Governance, and Interest on loans) reveals how the Western nuclear industry might improve going forward and why the use of the EEDB in the economic study presented here is largely appropriate. The time dependent costs, especially the accumulation of interest on private loans, make up the vast majority of the differences between the cost estimates and final price tag for recent nuclear projects. Whereas the overnight cost difference can largely be explained through regional variance in material and equipment costs between the UK and the US.

The long time-tables of western nuclear projects arise from four factors that are not present in the Eastern projects: the construction of first-of-a-kind reactors; incomplete design at the start of the project; the atrophying of supply chains; and an over-reliance on on-site, inexperienced construction teams [2]. There are also differences in financing (private vs public) and regulatory practices (interventionist vs hands-off) between the disappointments in the West and the successes in the East, but it is around fixing the issues of loss of tacit knowledge where the interest in small-modular reactors was born. This growing interest in SMRs and desperation for an economically viable fission power source in the West is best reflected in the shifting attitude of the Gen IV Technological Roadmap,the major

document guiding recent international nuclear research. In the 2002 initial publication, the forum could ”not resolve the debate” on the potential opportunity for economies of multiples to outweigh the economies of scale presented by the advocates of SMRs, and thus, little focus was put into SMRs as a research topic [4]. Meanwhile in the 2014 update of the Roadmap, an acknowledgement of the ” increased emphasis worldwide on the development and deployment of small modular reactors” came with the introduction of preliminary SMR designs in 4 out of the 6 reactor concepts that were highlighted for study.

The past decade has introduced a number of SMR concepts around the world based on the Light Water Reactor framework used in the vast majority of the operating Gen III plants. some of these, such as the Argentinean CAREM and the Russian KLT-40s, have entered construction and demonstration phase with others such as the US NuScale SMR joining them in the next couple years [5]. Along with the growth in the technical work, the body of work on SMRs economic, focused on their general economic viability. The economic promise of SMRs in reversing the skyrocketing growth in capital costs of current will theoretically be met by two-means. First, the simplification of key components and the integration of passive safety systems would directly lead to decreased unit construction costs. Second, the construction time for SMR plants would be dramatically reduced through the increased use of off-site, factory productions, allowed by the transportability and uniformity of smaller, modular systems, and the development of more robust supply chains and more experienced labor pool through the increased number of units required in place of gigawatt size units. The deployment of light water SMR units would open up opportunities for nuclear power to enter smaller and more remote electric markets, but the wide spread adoption of the SMR model will require the new designs to be economically competitive with large scale reactors. For the LWR based designs to be economically effective with low investor risk, the following conditions will have to be met on top of following through on the guarantee of multiple unit siting and serial construction; the acceptable return on investment is greater than 15%, the interest rates on debts is greater than 7% and

there are no great external delays in the installation of SMRs units [5]. These conditions relate to the fact that the potential cost competitiveness of SMR plants is nearly entirely dependent on the theory that they are associated with decreased construction costs.

1.3 The USMR Design

1.3.1 Objectives and the USMR Core

The objective of the high temperature, ultra-small modular reactor concept presented in this thesis, is to bridge the positives of both SMR and current large reactors in terms of economics so that the final design is cost competitve regardless of conditions. Typical to SMRs the modularity and simplicity of the design should allow for lower initial investment, and the multiple decades fuel cycle and high plant efficiency will keep the cost per kilowatt-hour competitive with large style plants. This concept should also be capable of efficient load following, and it may have the potential to provide ultra-high temperature process heat; areas in which traditional reactors have lacked. Current nuclear reactors have historically been ineffectual for load following - the variation of electrical output from a plant to match demand- largely due to the difficulty in rapidly changing power levels in a core and the amount of damage from thermal shock this can produce in core elements [6]. Beyond this, the vast majority of a traditional NPP's cost are sunk during construction, which makes it more economically efficient to use them as the base load, increasing the total electric output to spread the high costs. Modern reactors with outlet temperatures of around 300°C and even the proposed high-temperature reactors with outlet temperatures up to 700°C are unable to provide the process heat needed for many manufacturing tasks [7]. These temperature limits are largely imposed by the working fluids the reactors use for power transfer.

The potential for the USMR to outperform previous proposed SMRs designs is based on its utilization of a radically different method of electric conversion. Unlike nearly all other NPPs that rely on Rankine or Brayton cycles, this design takes advantage of the advances

in thermophotvoltaic (TPV) technologies over the last 25 years to convert the radiative heat from the reactor directly to electric power.[8] This departure from traditional heat cycles requires fundamental revision to the reactor core design, walkaway-safety systems, and operational parameters. Furthermore, the grid and energy markets of the future will be much more decentralize than today's in order to lower transmission losses and reduce risk of widespread outage, making it necessary to push towards smaller modular power units (1-100 MWe modular installations), with local distribution (e.g., micro-grids) even providing DC power for electric transportation. The nuclear power industry needs to be mindful of this potential future or risk becoming financially non-competitive in the changing markets.

To make the most of the high efficiency energy conversion of the TPVs, upwards of 50%, the outer emitter of the new reactor will have to maintain a temperature above 1300K. This means that the inner region of the core, by excluding internal coolant channels, may reach peak internal temperatures of 2300K . Therefore, this design is composed of high temperature material spread across five concentric, solid hexagonal blocks: inner graphite moderator, fuel material, outer graphite moderator, beryllium reflector, and tungsten emitter. The reactor is then cooled entirely via the radiation mechanism, which is possible with a fuel power density lower than 5 W/cm^3, producing an external heat flux comparable to the 100 W/cm^2 of a typical computer chip. Though operating at a significantly lower power density than the typical PWR, this solid design has enormous benefits. The simplified, modular solid block design means that the battery-type core design is a good candidate for advanced manufacturing techniques with greatly reduced manufacturing costs. The low power leads to a decades long cycle-length and, along with the lack of working fluid, makes the design extremely accident tolerant. Overall, the design promises high economic competitiveness with large scale reactors.

An illustration of the hexagonal concept is shown in Figure 1.2. The fuel meat (colored red) is completely enclosed with a cladding that provides fission product and fuel retention for the overall element. An outer graphite sleeve (colored gray) surrounds the fuel core to

increase the moderation power and reduce the fast neutron leakage. As neutrons slow, they pass the graphite layer and reflected back into the core. A radial neutron reflector (colored blue) and outer tungsten emitter (colored green) surround the core and serve to reduce the neutron leakage. The primary reactivity control system consists of polarly distributed control drums (pink color) within the innermost region of the core. One third of the drum's surface is coated with boron poison(brown color). Contrary to the control rods and fins in a typical LWR that are pulled out and inserted, these drums are rotated to increase or decreases parasitic absorption. Each drum covers a 60° arc length of the USMR core and can be rotated towards the fuel region increases the capture rate in order to suppress the reactivity and are brought all the way facing out for shutdown . Alternatively, rotating the drums away from the fuel region towards the center of the core decreases the probability of neutrons being absorbed by the poison instead of being reflected, resulting in a higher reactivity. In addition, the design includes emergency shutdown rods, similar to LWRs (denoted by the circular white voids). The use of control drums and emergency shutdown rods will allow for easy control of the reactor power under both normal and accident conditions.

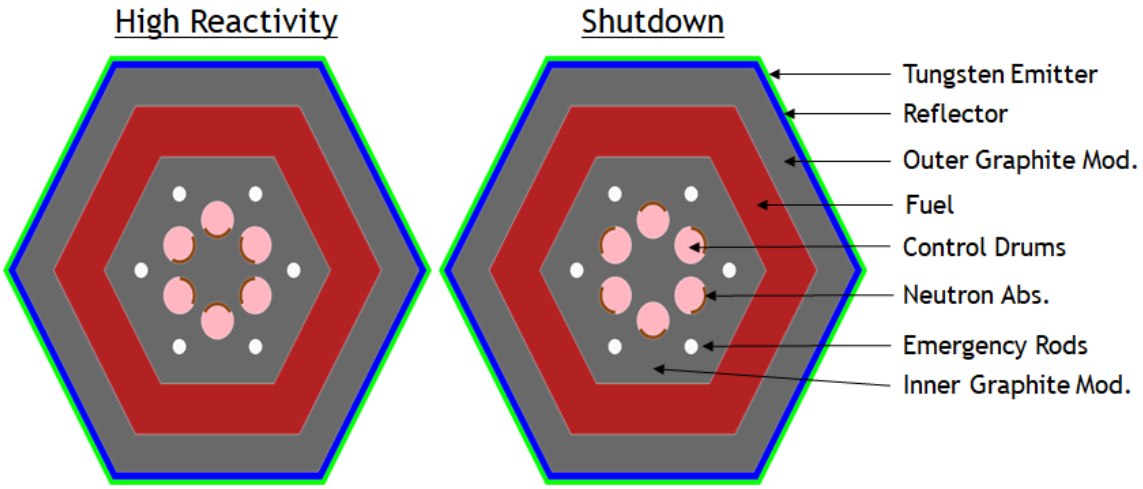

Figure 1.2. Radial configuration of the core with different control drums positions. The core is at operational mode when the neutron absorber facing interior (left figure) and at shutdown mode when the absorber facing exterior (right figure).

It worth noting that the model presented in Fig. 1.2 was not modeled explicitly for the

computational modeling presented chapters 3 and 5, but rather a more simplified model based on dividing the various regions to concentric cylinders was adopted, as described in Chapter 2. Such an approach allows to analyze thousands of cases and yet obtain a sense of the desired trends and trade-offs.

1.3.2 The Physics of the TPV

A key aspect to understanding the overall operation of the USMR design is to understand the physics underlying the coupling of the USMR core to the surrounding TPV panels. At high temperatures, the dominant form of heat transfer is through black-body radiation with a transfer rate that increases with surface temperature proportionally to T^4 as compared to convective heat transfer that is proportional to T. Having only atmospheric density air between the TPVs and core and no forced flow also helps ensure that the vast majority of heat is transmitted directly to the TPV, with a black-body spectrum given by Equation 1.1 and illustrated in Figure 1.3. Thermophotovoltaic materials are extremely useful in that they are typified by low energy thresholds for photon absorptions, as can be seen in Figure 1.3 along with the temperature evolution of the black-body spectrum. The figure thoroughly explains the requirement that USMR operate at temperatures significantly higher than a typical PWR, so that the dominating radiative heat transfer has a photon spectrum that largely falls in the absorption ranges of the typical TPV materials.

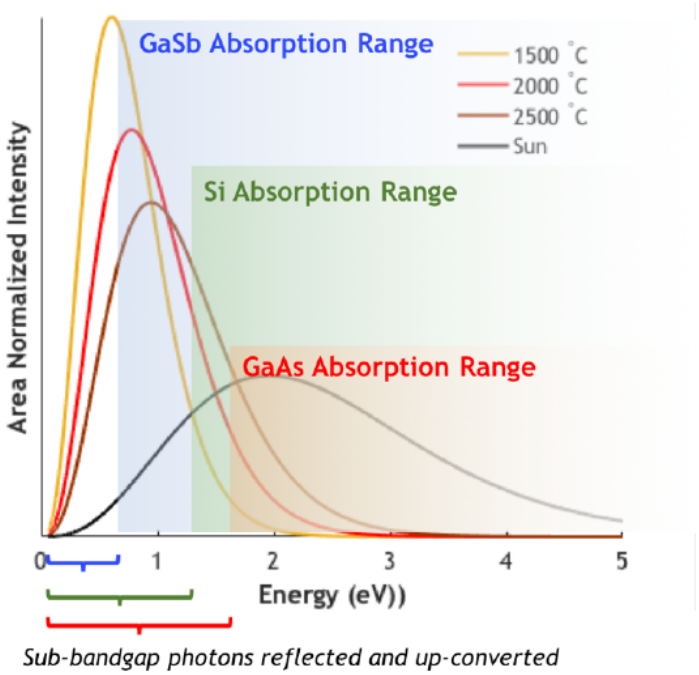

Figure 1.3. Black-body radiation spectrum and semiconductor absorption ranges.

$$f(v,T) = \frac{2hv^3}{c^2}\frac{1}{e^{\frac{hv}{kT}} - 1} \tag{1.1}$$

However, the overall system's efficiency of photon conversion can be maximized by reflecting photons that are not absorbed in energy band of the TPVs back towards the surface of the USMR, using highly (97-100%) reflective optical reflectors. The reflected photon flux works to maintain the tungsten surface temperature as it continues to radiate. Through this mechanic, shown schematically in Figure 1.4, minimal energy is lost by radiating to the surroundings. Figure 1.5 highlights the effect of the tungsten emitter temperature on the total efficiency of the system according to computational models [8].

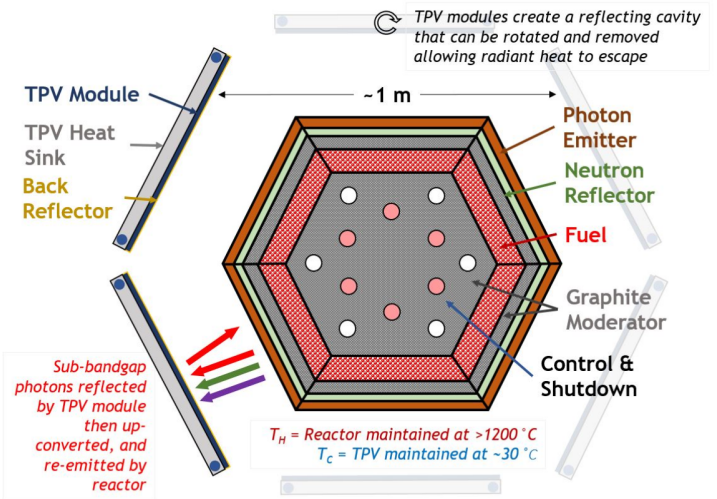

Figure 1.4. Schematic of the TPV and reactor coupled power block.

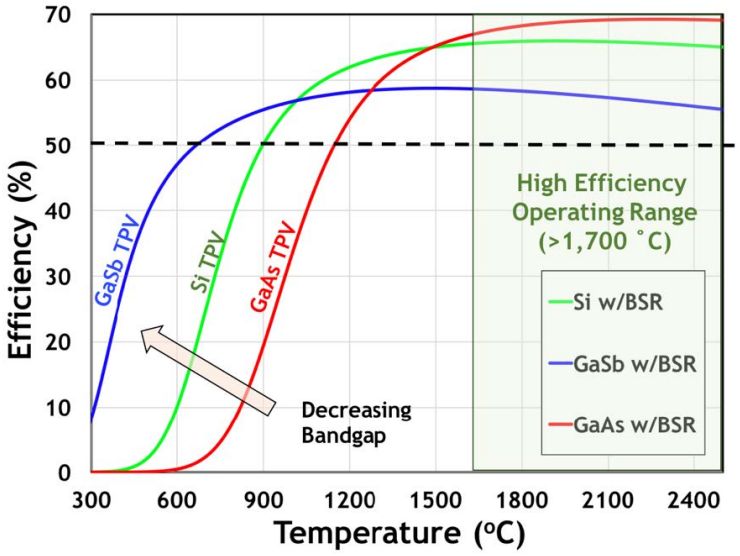

Figure 1.5. Measure of electric conversion efficiency of TPVs with a back surface photon reflector for an enclosed system from tungsten emitter.

Infrared photon flux is not the only incident radiation on the TPV surface. The mixed radiation field that is a product of the internal fission nuclear reaction has the potential to have a significant impact on the intrinsic TPV efficiency. Like all optical semiconductor devices, the TPV are vulnerable to current inhibiting damage due to transmutations of the base semiconductors and dopants through thermal neutron capture and lattice displacements from the fast neutron flux. To a degree, the TPV will self-repair some of the displacement damage

through isochronal annealing. A portion of the damage will be unrepairable and this will require that the TPV panels be replaced once they fall below an acceptable efficiency, in order to maintain the maximum output. Calculating the exact replacement rate of TPVs, which has the potential to prevent the viability of the project, requires experimental data on changing TPV efficiency in the radiation field of a thermal reactor, data that has not been measured yet. However, measurements have been taken on the efficiency of photovoltaic cells after exposure to 1 MeV electron and 10 MeV proton fluxes to simulate damage from unshielded cosmic rays [9]. Through the use of radiation quality factors, it is estimated that the TPV panels will likely need to be replaced every 2 to 5 years to maintain peak efficiency in the system.

1.4 Nuclear Energy Economics

1.4.1 Basic Economic Considerations

There are two main methods of comparison when evaluating the viability and economic competitiveness of the USMR. The first method is to examine the minimum price that a utility would have to sell the electricity produced a plant in order to break-even on the initial capital investment and the annual operating costs. This value is expressed as the Levelized Cost of Electricity (LCOE) [10]. LCOE is the sum of the investment, operation and maintenance (O&M), fuel and decommissioning costs- discounted back to present-value dollars using a discount rate, r, of 4.45%- normalized to the discounted total electricity (MWh) produced across the plant's financial lifecycle. This is represented in Equation 1.2, which can be simplified to the levelized capital costs added to the normalized annual costs under the assumption that the annual costs and electricity production remain constant.

$$LCOE = \frac{\sum_{i=0}^{N} \frac{CapitalCost_i}{(1+r)^i}}{\sum_{i=0}^{N} \frac{ElectricProduction_i}{(1+r)^i}} + \frac{AnnualCost_i}{ElectricProduction_i} \tag{1.2}$$

The second method is to determine the operational regime in which the USMR design

would be viable, if any, and compare the capital and annual costs of USMR to similar power sources. Throughout a given time period the demand and spot price of electricity will fluctuate with underlying predictable trends as well as random jumps, as illustrated in Figure 1.6 [11]. The minimum energy demand is met by baseload power plants. These types of plants, including generation III+ nuclear reactors, typically have higher capital costs but low operational costs; since the marginal costs make up only a small portion of their total costs, operating them at highest capacity is the most economic option. The predictable fluctuations in energy demand are met using mid-merit power plants, which include sources with mid-range capital and operation costs as well as older baseload plants with worsening efficiencies and growing operational costs. The random fluctuations are met by peak-load plants, such as combustion turbines, which have low initial costs and can be quickly activated, but also have high operational costs that discourage their frequent use.

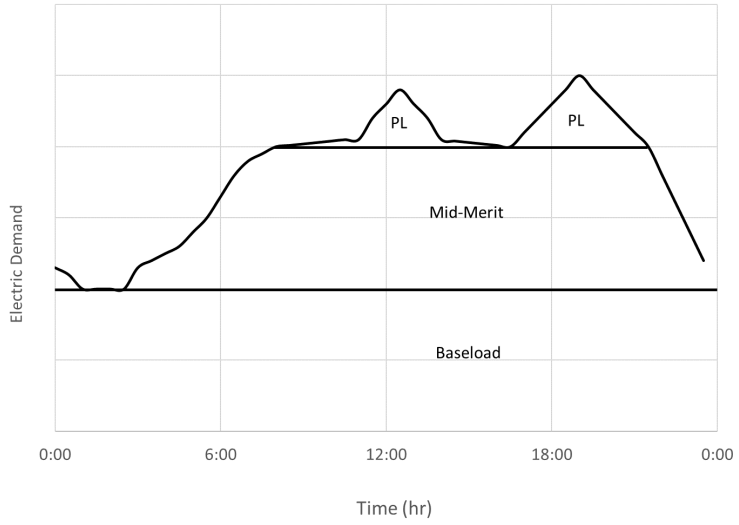

Figure 1.6. Simplified daily demand curve.

1.4.2 Law of Scale vs Law of Multiples

Across the United States' 60 nuclear power plants (NPP), there is a standard model of building large scale reactors (500 to 1300 MWe) utilizing Rankine and Brayton heat cycles to extract electrical power[12]. The motivation for these large-scale reactors is centered

on the economy of scale axiom. There is the expectation that the capital cost for a reactor grows slower than the reactor's electric generation capacity as the project grows [13]. Even the fuel cycle costs can potentially see decreases of 15 to 70% compared to smaller reactors. This desire for lower costs per kilowatt of electricity has driven the construction of reactors upwards of 1500 MWe in wealthier countries. However, not every state has the energy infrastructure that can handle these large additions of capacity or afford the large capital costs. Even the United States has been challenged by the skyrocketing cost overruns of the Plant Vogtle additions with the budget estimates jumping from $14.3B to over $27B. [14]

Despite sporting a competitive LCOE through low annual fuel and operating costs, interest in large scale, generation III+ nuclear power plants has waned dramatically. This has largely been due to the growing aversion towards large capital projects, which has invigorated the interest in small-scale, modular plants. However, the economies of scale suggest that the size of the plant does not linearly correlate with the cost of construction, and thus, the specific costs ($/MW) of SMRs could be much greater than those of a gigawatt reactor. The hope for SMRs is that the modularity of the units will allow for mass production of a single model which will improve the tacit knowledge of the manufacturers, leading to economic savings. In other words, the SMR gains in the law of multiples could potential outweigh the loss in the law of scale. The general formula for finding the relative specific cost of a plant using size scaling and production number scaling is given by Equation 1.3.

$$\frac{Specific\,Cost_i}{Specific\,Cost_0} = \left(\frac{Power_i}{Power_0}\right)^a * (1 - LR)^{\frac{ln(N)}{ln(2)}} \tag{1.3}$$

Where $Specific\,Cost_i$ and $Power_i$ are the specific cost and power of the design, i; a is the power scaling constant; LR is the learning rate in terms of percent savings in specific costs for doubling the number of units produced, and N is the number of units of the i design produced.

In the nuclear industry with a traditionally small learning rate, 5%, and high power scaling, -0.35, it would likely be necessary to quickly build many hundreds or thousands

of units of a particular SMR design to be competitive with larger plant sizes. For micro-reactors like the USMR, this number might even be higher. However, a regions energy grid has only so much capacity to expand in terms of both infrastructure and slowing demand growth. From March 2018 to March 2019, the electricity capacity of the US grew by only 16 GW [15]. So the major concern is how much additional capacity of a given size of a design is needed for the specific cost of that design to equal that of the reference, which can be given by the Equation 1.4.

$$Add.\,Capacity = Power_i * exp\left(ln\,(2)\,\frac{ln\left(\frac{Power_i}{Power_0}\right)^a}{ln\,(1-LR)}\right) \tag{1.4}$$

CHAPTER 2

COUPLED CONDUCTION-NEUTRONIC COMPUTATIONAL TOOL

Chapter 2 presents the development of the main computational design tool utilized in modeling the USMR design space for Chapters 3 and 5. A coupled conduction and neutronics solver sequence was developed that would rapidly converge on the power profile, temperature profile, and reactivity curve for a given design. This process included the development and validation of a finite conduction solver, the creation of Serpent neutronic models and a sequencing scheme.

2.1 Conduction Model

2.1.1 Finite Element Conduction Solver

This section describes the finite difference model [16] used to solve the steady-state conduction model. The formulation relies on the resistance model, according to which the temperature in each node *i* is obtained by considering the heat transfer between multiple adjacent nodes. Denoting the node of interest as *i* and the adjacent nodes as *j*, we can find the temperature in node *i* using the following relation:

$$T_i = \frac{q_i + \sum_j \frac{T_j}{R_{ij}}}{\sum_j \frac{1}{R_{ij}}} \tag{2.1}$$

where, q_i is the heat produced in node *i*, and R_{ij} is the resistance between the nodes *i* and *j*. In the framework of our analysis, the resistance can take the form of conduction or convection (radiation included). In our analysis, each node *i* has only two adjacent neighbors, *i.e.*, left (R_{i-}) and right (R_{i+}) resistances.

The cylinder is discretized into radial layers with thicknesses of $\triangle r_i$. The volume of

element *i* is $\triangle V_i = r_m \triangle r_i \triangle \phi \triangle z$. The heat produced in a specific layer *i* is calculated by taking the product between the power density and the corresponding volume in layer *i*.

In cylindrical coordinate system, the conduction resistances are calculated according to Equation 2.2.

$$R_{i\pm} = \frac{\triangle r_i}{\left(r_m \pm \frac{\triangle r_i}{2}\right) \triangle \phi \triangle z} \frac{1}{k_{i\pm}} \tag{2.2}$$

It must be pointed out that for the outermost node (*i.e.*, $i = N$), the resistance term is slightly modified due to the shorter distance to the boundary as follows:

$$R_{N+} = \frac{\triangle r_N/2}{\left(r_m + \frac{\triangle r_N}{4}\right) \triangle \phi \triangle z} \frac{1}{k_{N+}} \tag{2.3}$$

Combining all these relations, the tri-relation can be written in a matrix form as seen in Equations 2.4, 2.5, 2.6, and 2.7.

$$R^{-1} * T = Q \tag{2.4}$$

$$R^{-1} = \begin{bmatrix} \frac{1}{R_{1-}} + \frac{1}{R_{1+}} & -\frac{1}{R_{1+}} & 0 & 0 & \cdots & 0 \\ -\frac{1}{R_{2-}} & \frac{1}{R_{2-}} + \frac{1}{R_{2+}} & -\frac{1}{R_{2+}} & 0 & \cdots & 0 \\ \vdots & \cdots & \ddots & \ddots & \cdots & \vdots \\ 0 & \cdots & 0 & -\frac{1}{R_{(N-1)-}} & \frac{1}{R_{(N-1)-}} + \frac{1}{R_{(N-1)+}} & -\frac{1}{R_{(N-1)+}} \\ 0 & \cdots & 0 & 0 & -\frac{1}{R_{N-}} & \frac{1}{R_{N-}} + \frac{1}{R_{N+}} \end{bmatrix} \tag{2.5}$$

$$T = \begin{bmatrix} T_1 \\ T_2 \\ \vdots \\ T_{N-1} \\ T_N \end{bmatrix} \tag{2.6}$$

$$Q = \begin{bmatrix} q_1 \\ q_2 \\ \vdots \\ q_{N-1} \\ q_N + \frac{T_w}{R_{N+}} \end{bmatrix} \tag{2.7}$$

Here the outer temperature of the emitter, denoted by T_w, remains at a constant wall temperature (e.g., 1500°C) due to the isolation of the reactor core. In order to account for the temperature-dependent conductivities, the implementation relied on an iterative scheme, in which the conductivities were initially guessed according to a nodal uniform temperature distribution [T_1 T_2 $\cdots$ T_N]^T = T_w. Once, the nodal temperature distribution is obtained, it is reapplied to update the conductivity values and hence the resistances. This iterative procedure continues until a convergence of $\triangle T_i < 0.5$°C in all nodes i is satisfied.

2.1.2 Material Properties

The material selection was constrained by the high operating temperatures of the core. Table 2.1 reports the materials composition, mass density, ρ, and melting/sublimation temperature, T_m, with the enriched tungsten isotopic composition given in Table 2.2. In this study a 19.75 $\%$ U^{235} (by weight) was used. Table 2.3 presents the temperature-dependent thermal conductivity k. For UN, UC, UC_2, (U,Zr)C the equations describing the thermal conductivity are valid in the range of [1000, 2800]K, while for UO_2 and graphite, the correlations are valid in the intervals [250, 1800]K and [500, 1800]K, respectively. Outside

these ranges, k retains a constant value, matching the closest value in the range of validity.

In this paper, the following simplifications are carried out:

- Due to the preliminary nature of this analysis, the effect of porosity, and temperature on the mass density is neglected.

- The CERMET fuel is composed of UO_2 particles embedded in a tungsten matrix. The thermal conductivity of the composite fuel, k_c, is calculated with the Bruggeman–Fricke methodology, based on the hypothesis of spherical fuel particles [17]

$$k_c = k_p + (1 - V_p)(k_m - k_p) \left(\frac{k_c}{k_m} \right)^{\frac{1}{3}} \tag{2.8}$$

  In Equation 2.8, k_m and k_p denote the thermal conductivity of tungsten and UO_2 respectively, while V_p represents the volume fraction of fuel particles.

- The CERMET fuel melting temperature is calculated using the same relation presented in Equation 2.8, but with temperatures rather than conductivity values of tungsten and UO_2.

- The melting temperature, in Kelvins, for the uranium mononitride, UN, is obtained from the following equation:

$$T_m = 3035 \cdot p_{N_2}^{0.02832} \tag{2.9}$$

  In Equation 2.9, p_{N2} denotes the partial pressure of nitrogen in atmosphere. If P_{N2} is the nitrogen partial pressure in Pascal, the following empirical correlation can be utilized [18]:

$$\log(P_{N2}) = \left(6.8216 + 1.882 \cdot 10^{-3}\, T - \frac{23543.4}{T} \right) \tag{2.10}$$

Since the analyzed reactor core exhibits temperatures above 1,000 K, the nitrogen partial pressure is strictly larger than unity. Therefore, a conservative estimate of the melting temperature of 3035 K was imposed here.

- Weight loss phenomena, caused by the disassociation of uranium and nitrogen and the evaporation of metallic uranium at high temperature, are not analyzed.

- The thermal conductivity of enriched tungsten is assumed to match the one of the natural element.

Table 2.1. Mass density, ρ and melting/sublimation point, T_m for various materials.

Materials	ρ, **g/cm**^{3}	$\mathbf{T_m}$ **,K**
UO_2	10.97	3138
UN	14.32	3035
UC	13.63	2798
UC_2	11.28	2710
(U,Zr)C	3.49	3100
Graphite H-451	1.74	3652
Enriched Tungsten	19.25	3667
Natural Tungsten	19.25	3667

Table 2.2. Composition of the enriched tungsten used in this study.

Isotopes	**Isotopic Weight Fraction,%**
W^182	1.6
W^183	10.0
W^184	87.0
W^186	1.4

Table 2.3. Materials' thermal temperature-dependent conductivity correlations and references.

Materials	**Reference**	**Thermal Conductivity**, W/m/K
UO_2	[19]	$10.41 - 9.44 \cdot 10^{-3} \cdot T + 2.52 \cdot 10^{-}6 \cdot T^2$
UN	[17]	$1.864 \cdot T^{0.361}$
UC	[20]	23.8
UC_2	[20]	18.0
(U,Zr)C	[21]	30.0
Graphite H-451	[22]	$3.28248 \cdot 10^{-5} \cdot T^2 - 1.24890 \cdot 10^{-1} \cdot T + 1.69245 \cdot 10^2$
Tungsten	[17]	$-35.911 \cdot \log(T) + 373.062$

The temperature-dependent conductivity for the various fuels are plotted in Figure 2.1. It is noticeable that the CERMET conductivity, for low level of fuel loading, *i.e.*, below 20%, is considerably higher than all the other fuel types. This makes the CERMET fuel, the best choice when Highly Enriched Uranium (HEU) is available. However, this advantage diminishes more fuel introduced in the cermet. For all the cases analyzed in this paper, it was chosen to fix the fuel enrichment to 19.75 wt%, allowing to maximize the system compactness, while benefiting from the use of Low Enriched Uranium (LEU). In fact, the utilization of LEU not only reduces the cost associated with the enrichment process, but it is also consistent with the US government policy that aims to minimize the use of high-enriched uranium for civilian purposes.[23]

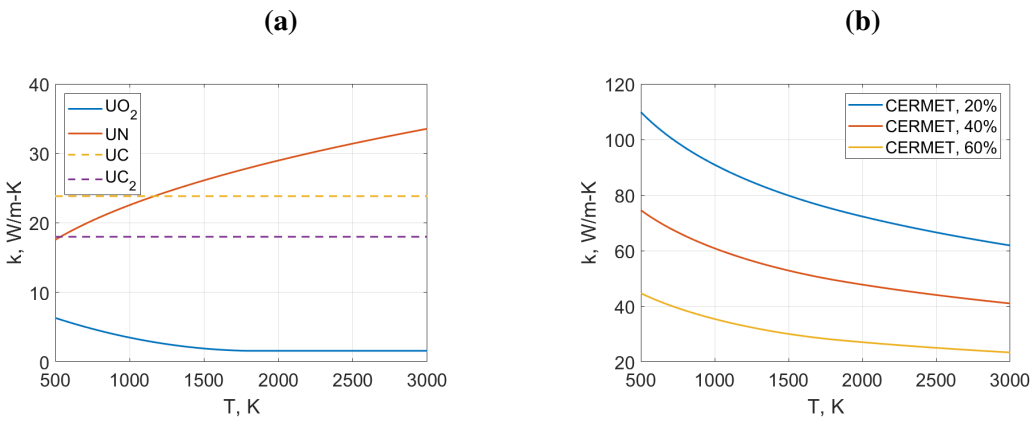

Figure 2.1. Temperature-dependent thermal conductivity: (a)UO_2, UN, UC, and UC_2, (b) CERMET fuel types.

2.1.3 Code Validation

An arbitrary selected case used to validate the conduction solver is presented here as described in Table 2.4 and illustrated in Fig. 2.2. The test case relies on a four concentric rings with non-uniform heat distribution and slightly different conductivity values. The numerical solution of the test problem, obtained by discretizing the geometry, is compared to the analytical solution in Fig. 2.2.a. As noticeable, the lines are nearly indistinguishable. The maximum percent error is 0.0006%.

Table 2.4. Four-Ring Test Case Specifications.

Ring	**Radius**, cm	**Conductivity**, $W/m\ K$	**Heat Generation**, W/cm^3
1	10	10	0
2	20	10	1
3	30	10	0
4	33	1	0

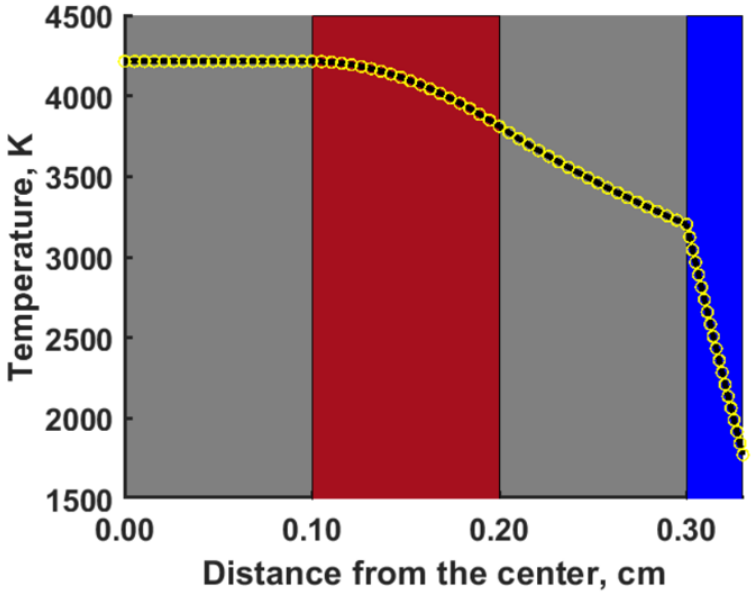

Figure 2.2. Comparison between analytic (yellow circles) and numerical (solid black line) temperature distributions.

2.2 Serpent Neutronics Model

Serpent is a multi-purpose, three-dimensional, continuous-energy Monte Carlo particle transport code, developed at VTT Technical Research Centre of Finland, Ltd. [24] The software provides accurate and efficient results for depletion, burnup, power profile, and other neutronic related phenomena. The code relies on Woodcock delta-tracking for particle transport as well as typical surface tracking, and it provides a fine distributed energy grid for its analysis. Serpent also features a built-in depletion calculator based on the Chebyshev Rational Approximation Method.

Thousands of combinations of materials, dimensions, center-line and surface temperature were analyzed for the studies in Chapters 3 and 5. To obtain a preliminary refinement of the design space, as seen in Chapter 3, it was here decided to deploy a volume/mass-conserving axisymmetric cylindrical model composed of four layers: (1) Inner graphite, (2) Fuel, (3) Outer graphite, and (4) Tungsten emitter. The design study conducted in Chapter 5 incorporated a set, 1 cm thick BeO reflector, but the effect of dimensionally varying the radial BeO reflector is not presented in this thesis. A general radial view of this domain is

shown in Figure 2.3. Each neutronics model was run using 50,000 particles for 200 cycles, with 50 inactive cycles; these population statistics were chosen because they led to effective criticality uncertainties of under 50 pcm.

Under the following assumptions, the trends drawn from the design space of the simplified, four-ring, cylindrical model can inform design decisions for more exact study of the USMR core.

- The axial length is much greater than the total radial dimensions, *i.e.*, meters versus centimeters, and therefore the axial component of the gradients will be negligible with respect to the radial.
- A core with a hexagonal cross-section is similar enough to a cylindrical cross-section that the general behaviors of the design under variation of dimensions and temperature follow the same pattern, even if the exact optimum values differ slightly.
- The reactivity worth of the beryllium oxide reflector is approximately fixed to its thickness, and therefore an optimization of reflector thickness can be performed separately from this initial examination of the moderator and fuel dimensions.

2.3 Conduction-Neutronic Coupling Scheme

A linkage script was written to couple Serpent with the conduction model, described in Section 2.1 to perform coupled thermal-neutron transport analysis. The coupling between Serpent and the conduction calculations relies on iterating on the power and temperature fields until very small variation in temperature is observed (i.e., maximum local/nodal variation is below $0.5°$C).

Different mesh discretization was used for the neutronic and thermal models, as shown in Figure 2.3. For the neutronic modeling, Figure 2.3a, a coarse mesh is applied, according to which, each region is characterized by a single temperature value. However, the fission power shape is obtained by dividing the fuel ring into 20 equal-volume concentric rings,

where the power is tallied. For solving the conduction problem a very fine mesh, Figure 2.3b, is applied ($\triangle r$ is on the order of mm). The mapping of power from the neutronic to the thermal mesh is performed by the linkage code. In addition, the condensation procedure to average the fine temperature distribution to unique moderator, fuel, and emitter temperature values is also performed by the linkage code.

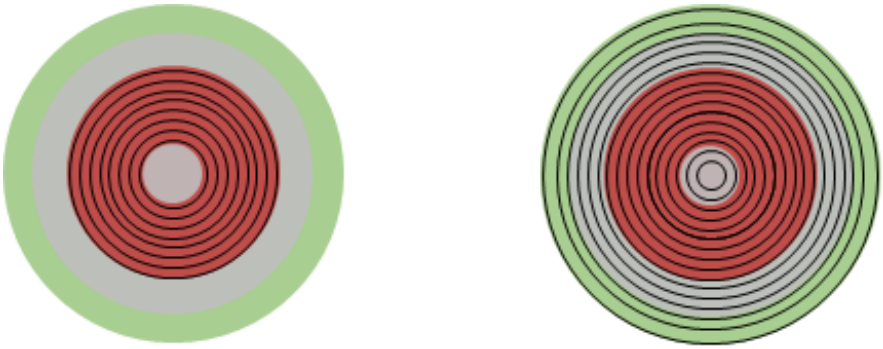

(a) Neutronic mesh. **(b)** Thermal mesh.

Figure 2.3. Schematic view of the mesh types used in the neutronic and thermal models. The inner and outer graphite moderator is indicated by the grey color, the red ring is the fuel, and the tungsten emitter is indicated by the green color.

The iterative sequence that was used in this study to derive converged thermal and neutronic solutions can be seen in the chart in Figure 2.4. In the current study 2–3 iterations between Serpent and the conduction model were sufficient to converge on the power and temperature distributions.

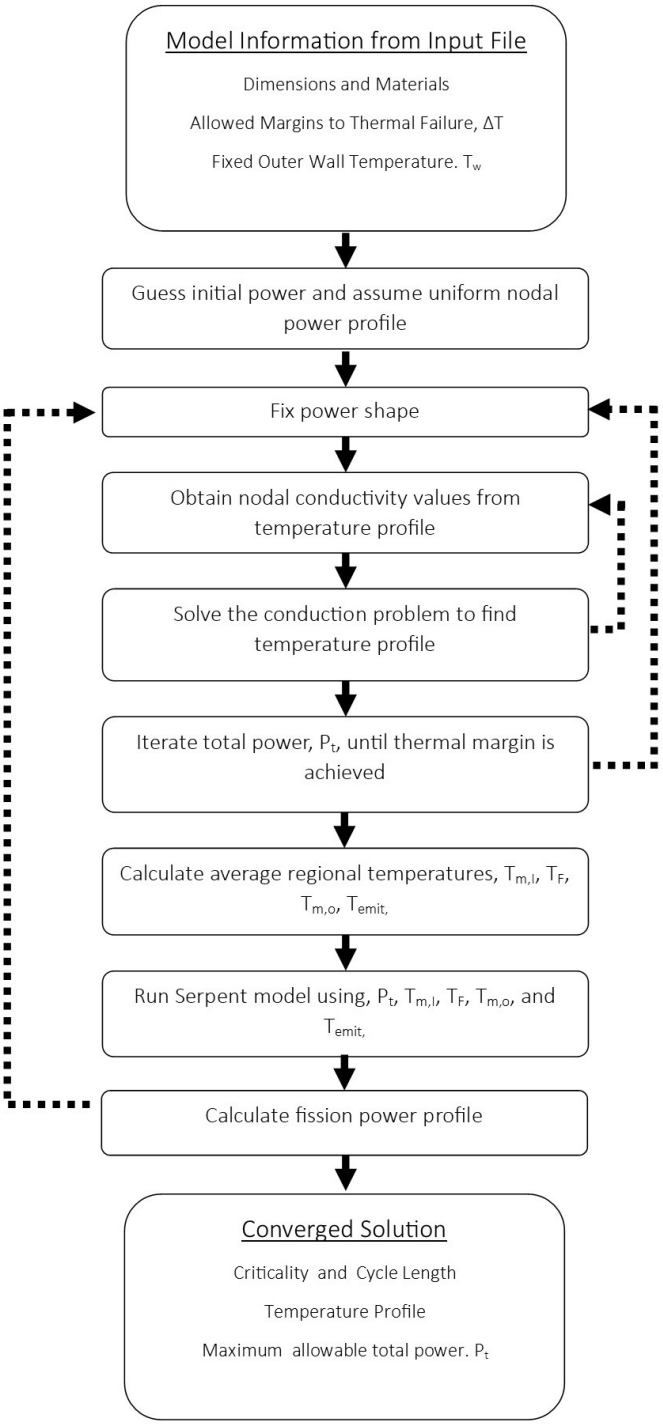

Figure 2.4. Flow chart of the iterative sequence to couple Serpent and the thermal feedback.

CHAPTER 3
PRELIMINARY DESIGN STUDY

3.1 Basis

The preliminary sampling of the design space aimed to find an ideal set of materials and dimensions for the new reactor concept. This study assumed a steady-state, beginning of life framework to examine design cases for a selection of five fuels:uranium carbide, uranium dicarbide, uranium nitride, uranium-zirconium carbide and CERMET fuel. The external surface temperature, T_s, and the margin to thermal failure (margin to melting), ΔT_c, were varied parametrically for each fuel type. The variation range is $[1300, 1700]^{\circ}$C and $[50 - 600]^{\circ}$C for T_s and ΔT_c, respectively. For each combination of $\{\Delta T_c, T_s\}$ and fuel-type, sensitivity analyses were performed by varying the inner/outer graphite moderator and fuel dimensions. The radial thickness of the tungsten layer was arbitrary fixed to 0.5 cm. For each of these points in the design space, the maximum achievable power density, p, and the effective multiplication factor were iteratively calculated with the coupled sequence described in Section 2.3. The desired outcomes of this initial analysis were:

- An optimum design point for each combination of fuel type, external surface temperature and margin to thermal failure is found. This is defined as the combination of radial dimensions giving a critical system with the maximum power density.

- The locus of the optimal cases is identified as a function of external surface temperature, margin to thermal failure, and power density.

- The most promising fuel candidates for the purpose of building the ultra-high temperature modular reactor is found by comparing the highest achievable power density without thermal failure and the greatest system compactness.

In the remainder of this chapter, selected results for each fuel type are presented. A summary of the results and comparison among the different fuel types in Section 3.3. This is followed by a short depletion analysis of the ideal design for uranium nitride and uranium carbide and the conclusions drawn from the preliminary design analysis.

3.2 Results

3.2.1 Uranium Carbide

The uranium carbide fuel is characterized by high thermal conductivity and melting temperature that reach $\tilde{2}800$ K [20]. Figures 3.1.a and 3.1.b show the criticality eigenvalue and the power density as a function of the system dimensions for T_s=1500°C, and ΔT_c=200°C, respectively. This trend is representative of any boundary condition choice. In the figure, inner, intermediate, and outer region denote the thickness of the inner graphite, fuel layer, and the the outer graphite layer, respectively. As expected, the power density decreases with increased system dimensions; however, increasing dimensions improves criticality through decreasing leakage. The optimum case for this choice of boundary conditions has an external radius of 25.94 cm.

The locus of the optimal cases is plotted in Figure 3.1.c as a function of the boundary conditions. The power density is opposite to the temperature difference between center-line temperature and external surface temperature. As noticeable from Figure 3.1, UC achieves power densities higher than 1 W/cm^3, even when a margin larger than 300°C to thermal failure is chosen.

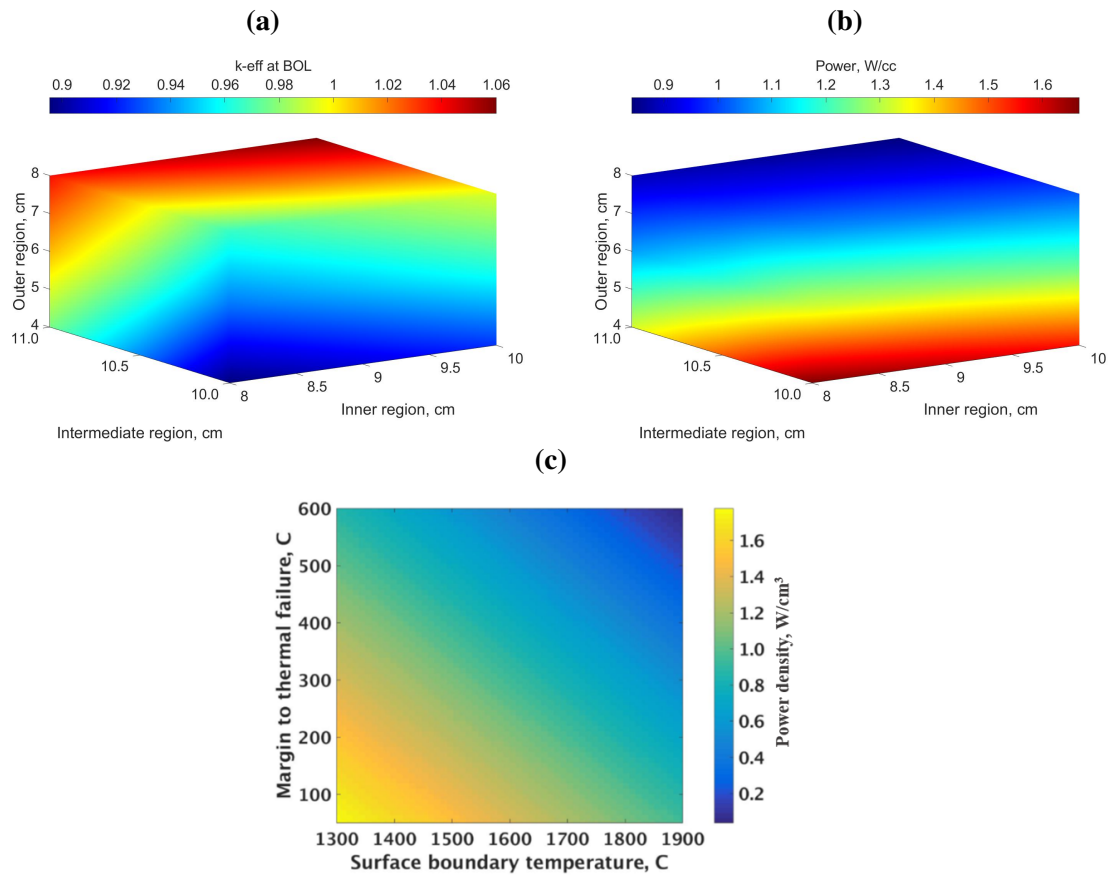

Figure 3.1. Selected results for uranium carbide: (a) Criticality eigenvalue design-space distribution for T_s = 1500^{o}C and ΔT_c=200^{o}C. (b) Power density design-space distribution for the same boundary conditions. (c) Power density of optimum case as a function of boundary conditions.

3.2.2 Uranium Dicarbide

Uranium di-carbide (UC_2) has a higher moderator-to-fuel ratio, which might be beneficial from neutron economy [20] . However, its lower conductivity, melting temperature, and mass density compared to UC (Section 2.1.2) leads to a lower power density, and a larger critical radius as shown in Figure 3.2.

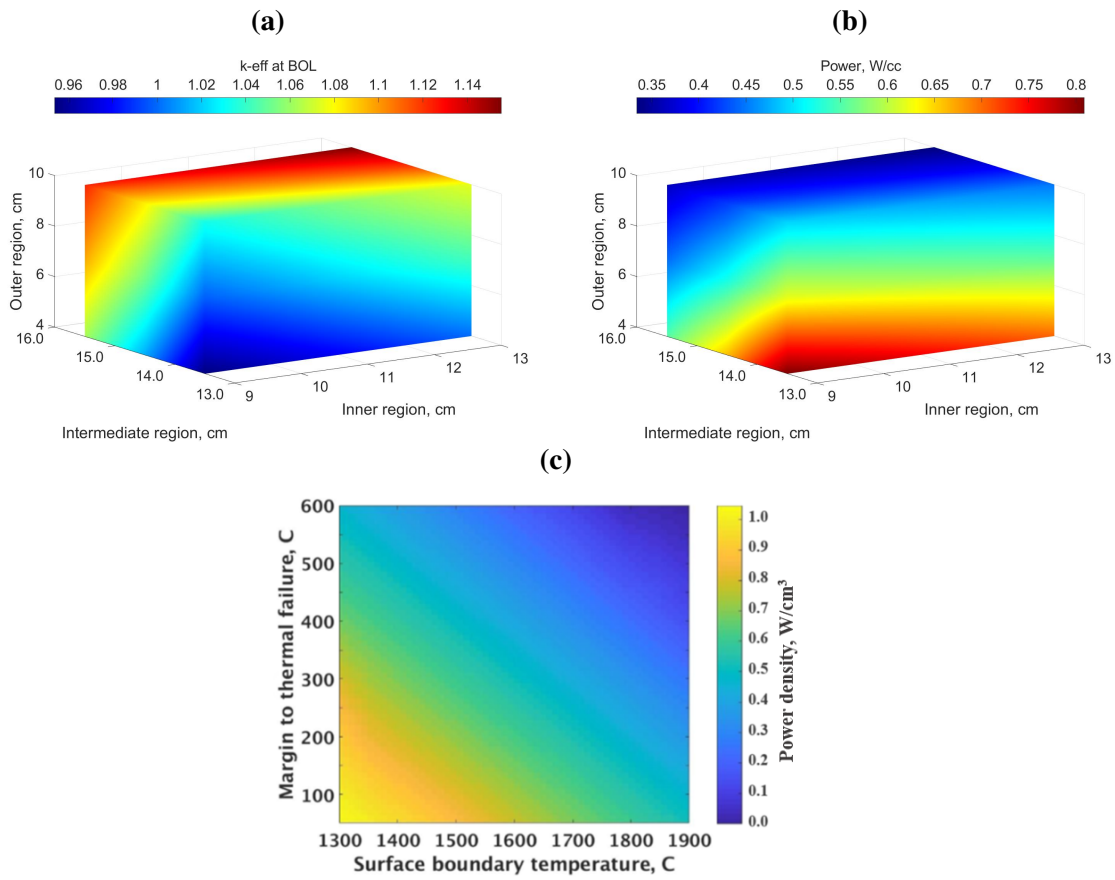

Figure 3.2. Selected results for uranium carbide: (a) Criticality eigenvalue design-space distribution for T_s = 1500^{o}C and ΔT_c=200^{o}C. (b) Power density design-space distribution for the same boundary conditions. (c) Power density of optimum case as a function of boundary conditions.

3.2.3 Uranium Nitride

Among the selected fuels, the uranium mono-nitride (UN) has the highest mass density and conductivity [17]. Its melting point is more than 300 K higher than the binary carbide fuels. As noticeable from Figure 3.3, this leads to higher power density compared to UC and UC_2. However, the system is less compact. In fact, thicker graphite rings are needed to compensate for the difference between nitrogen's and carbon's moderating ratios. The outer radius, as computed by the coupled thermal-neutronic analysis is 31.48 cm.

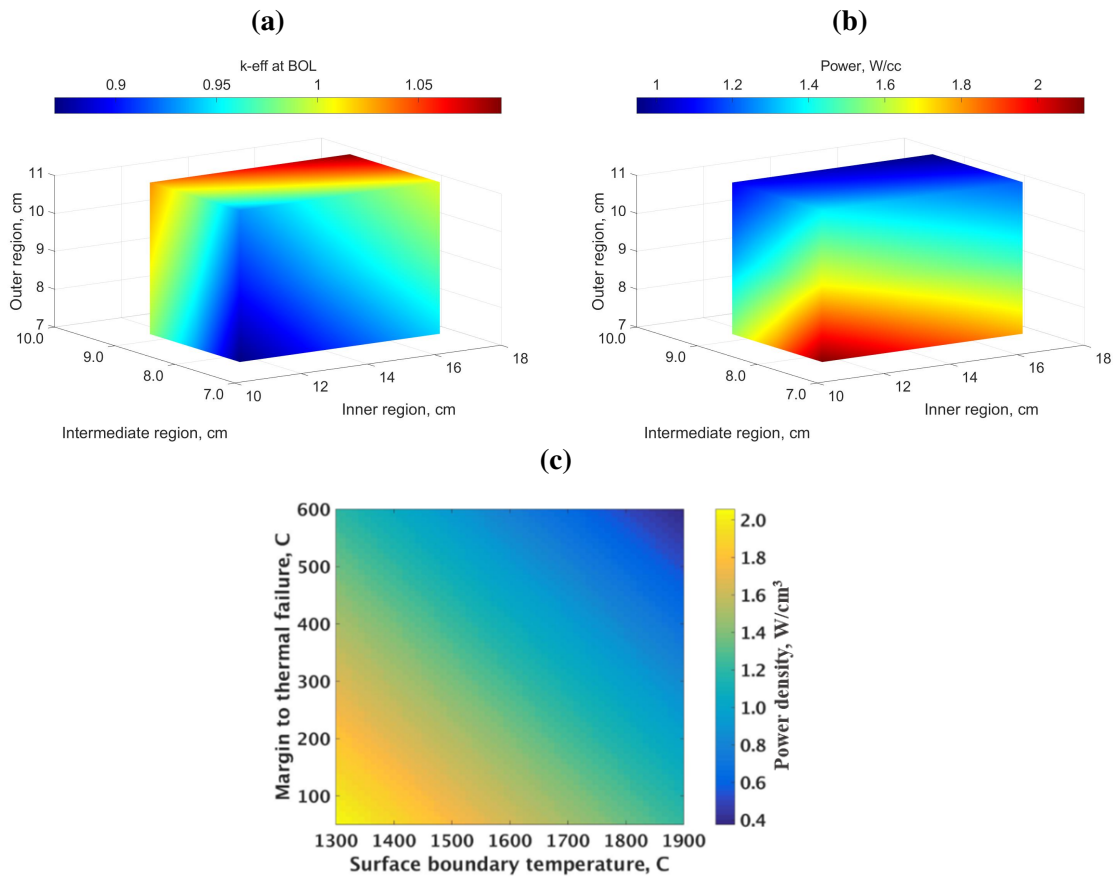

Figure 3.3. Selected results for uranium carbide: (a) Criticality eigenvalue design-space distribution for T_s = 1500^{o}C and ΔT_c=200^{o}C. (b) Power density design-space distribution for the same boundary conditions. (c) Power density of optimum case as a function of boundary conditions.

3.2.4 Uranium-Zirconium Carbide

Uranium Zirconium Carbide (UZrC) was first developed for nuclear-enabled space flights [21]. It is characterized by high melting temperature and thermal conductivity. Lower density makes it ideal for aeronautics application, but it can be a disadvantage when LEU is utilized, since a lower fissile loading leads to higher critical dimensions, and thus lower power density.

The power density trend is illustrated in Figure 3.4.a. It can be noticed the low power density as compared with UC, UC_2, and UN. The outer radius for the optimal case is 122.12 cm, about four times the dimensions of the UC_2-fueled system.

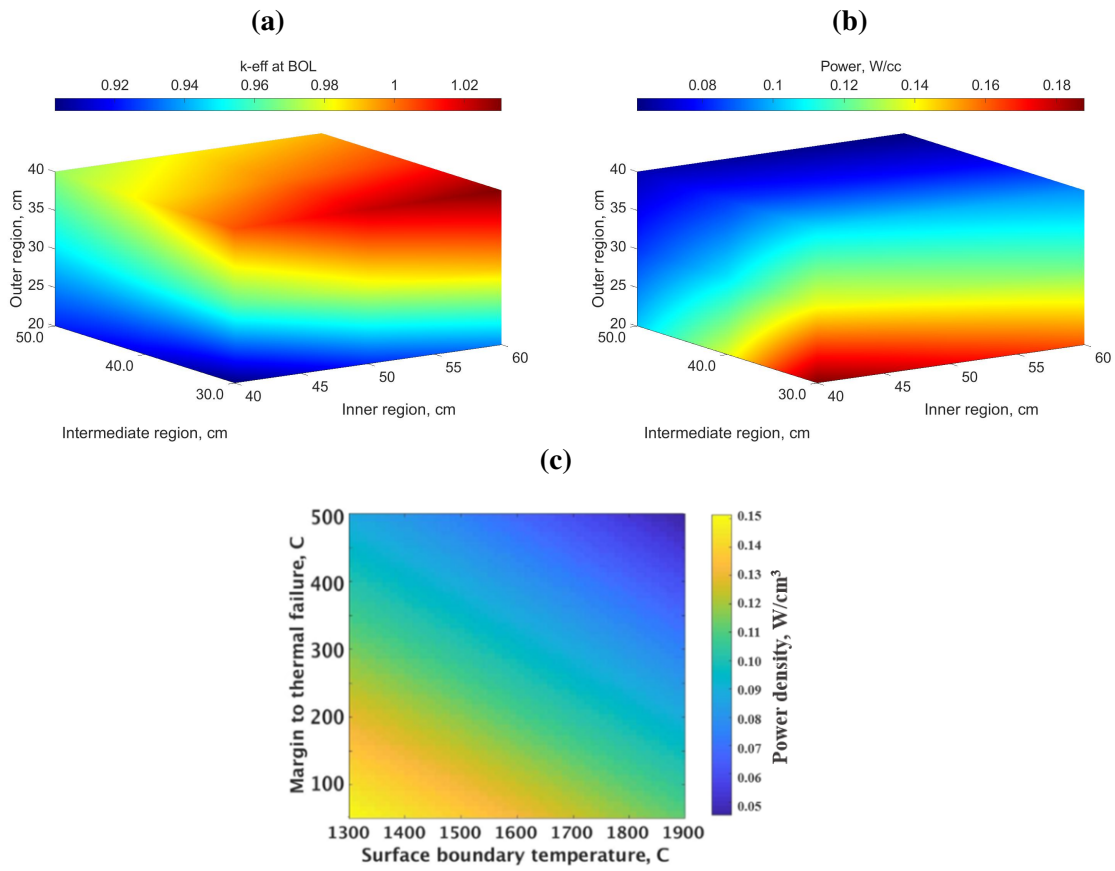

Figure 3.4. Selected results for uranium carbide: (a) Criticality eigenvalue design-space distribution for T_s = 1500^{o}C and ΔT_c=200^{o}C. (b) Power density design-space distribution for the same boundary conditions. (c) Power density of optimum case as a function of boundary conditions.

3.2.5 CERMET fuel

CERMET fuel was first developed for space-flight applications [23]. The fuel is composed by UO_2 particles embedded in a tungsten matrix. This gives the material outstanding thermal and structural properties. However, from a neutronic standpoint, the CERMET fuel presents unique challenges. In fact, all the naturally occurring tungsten isotopes present non-negligible thermal capture cross-section. Among these isotopes, the one with minimum cross-section is ^{184}W. In this study, it is supposed the fuel to be enriched to 80% in ^{184}W. This is compatible with the levels achievable through gas centrifuges. [23] Higher tungsten enrichment values are not considered for economical reasons. A 60% fuel to

uranium-to-tungsten ratio is utilized.

The power density trend for the CERMET fuel is reported in Figure 3.5. The system external radius is 82.52 cm; in excess of three times the outer radius of the UC-fueled reactor. The system is also characterized by lower power density, similar to the UZrC case.

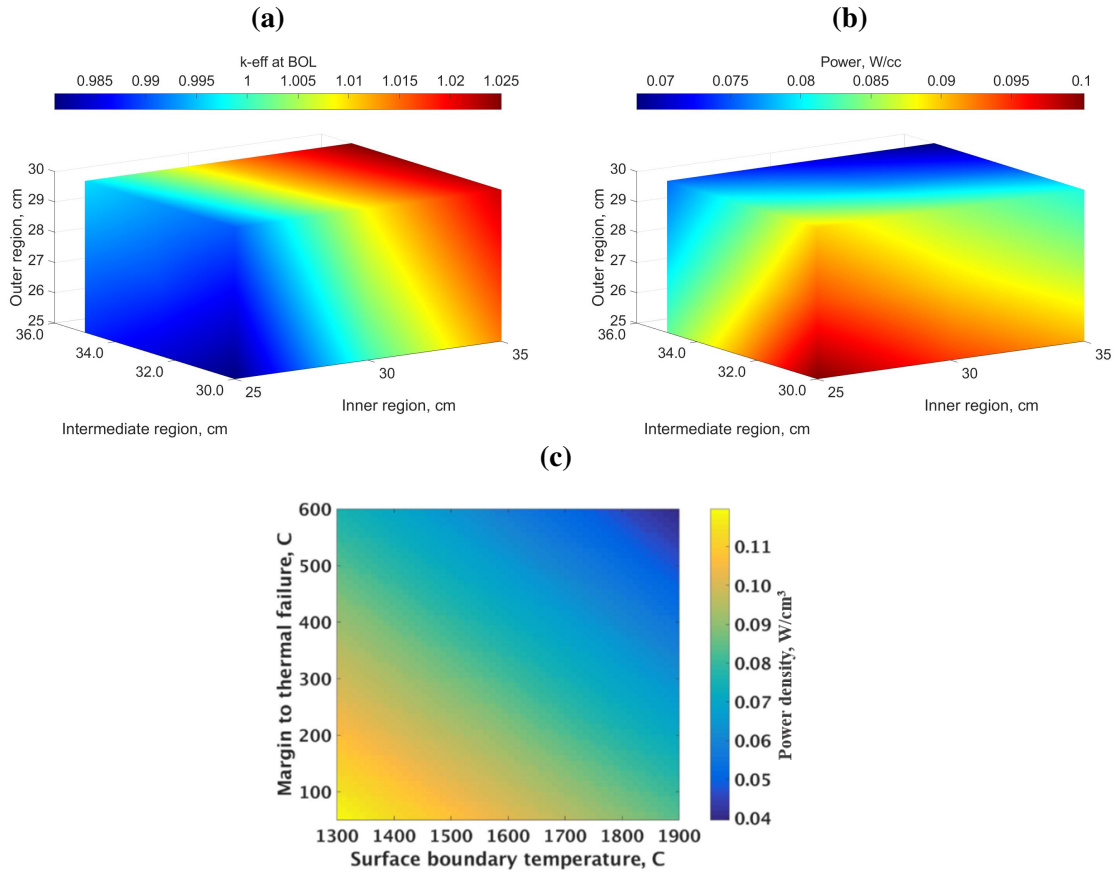

Figure 3.5. Selected results for uranium carbide: (a) Criticality eigenvalue design-space distribution for T_s = 1500^{o}C and ΔT_c=200^{o}C. (b) Power density design-space distribution for the same boundary conditions. (c) Power density of optimum case as a function of boundary conditions.

3.3 Summary

In this Section, selected results of the steady-state sensitivity study are presented. The following considerations can be drawn from the analysis:

- The adoption of UC and UC_2 lead to more compact design. However, the achievable power density is limited by the fuel's density and melting temperature.

- UN allows to obtain the maximum power density. However, the reactor's dimensions must be increased to achieve higher levels of neutrons' moderation.
- UZrC and CERMET fuel are not ideal choices for this reactor type, due to the large critical dimensions and the low power density.

The system's dimensions and power density are reported in Table 3.1 for $T_s = 1500°C$ and $\Delta T_c = 200°C$. A Figure of Merit (FOM) normalized to the FOM value for UC_2 is defined to compare the different fuel types:

$$FOM = \frac{p}{R_{out}} \tag{3.1}$$

In Equation 3.1, R_{out} is the external radius, while p denotes the power density. The table is representative of every combination of boundary conditions, since the same trends are followed by all the fuel types.

Table 3.1. Dimensions and power density for different fuel types for $T_s = 1500°C$ and $\Delta T_c = 200°C$. R_1: radius of inner graphite layer. R_2: external radius of fuel ring, R_3: external radius for outer graphite ring.

Fuel	R_1, cm	R_2, cm	R_3, cm	$p, W/cm^3$	R_{out}	FOM
UC_2	9.12	16.68	4.00	0.70	29.78	1.00
UC	10.00	11.94	4.00	1.24	25.94	2.02
UN	13.99	10.50	7.00	1.54	31.48	2.07
UZrC	40.00	49.80	32.32	0.12	122.12	0.04
Cermet, 60%	25.00	32.53	25.00	0.09	82.53	0.05

3.4 Preliminary Depletion Analysis

Preliminary depletion analyses were conducted for the two most promising fuel types, uranium carbide and uranium nitride. The dimensions for the optimal critical case for each fuel type with an outer boundary condition of 1500^oC and a marginal temperature of 200^oC

were taken. Additional reactivity worth was added to push the cases above criticality by including 0.5 cm of beryllium oxide reflector between the outer graphite and the tungsten regions in the simplified core models. Table 3.2 presents the radial dimensions for these two cases as well as the initial multiplication factor.

Table 3.2. Depletion study case dimensions.

Parameter	**UN Value**	**UC Value**
Inner Graphite Radius, cm	17.5	10.0
Fuel Radius, cm	26.5	22.0
Outer Graphite Radius, cm	33.5	26.0
Beryllium Reflector Radius, cm	34.0	26.5
Tungsten Filament Radius, cm	34.5	27.0
Initial Criticality for 200°C Margin	1.0135	1.0165

The same iterative model (Section 3.1) was run while only (T_c was fixed to 1500°C) varying the marginal temperature. A converged power and temperature profile was found for each case using the coupling scheme which was then used to deplete the cases until they reached criticality allowing for single batch cycle length and burnup to be calculated. As can be seen, the greater the marginal temperature requirements, the greater the cycle length. This is of no surprise since the maximum operational power density decreases with increasing core size. The results of studying discharge time, burnup and total linear power variation with safety margin temperature can be found in Figure 3.6 for uranium carbide and Figure 3.7 for uranium nitride.

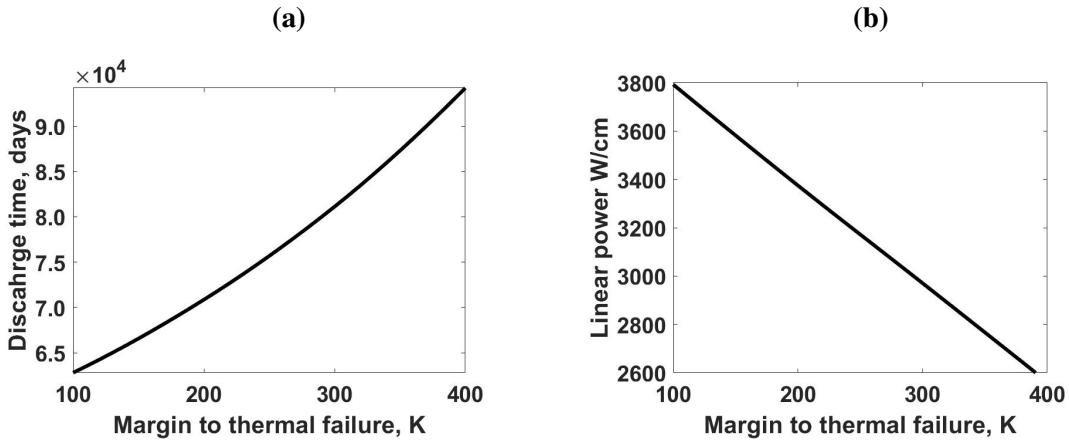

Figure 3.6. The Discharge Time(a) and Linear Power(b) for uranium carbide fuel core at an outer temperature 1500^oC.

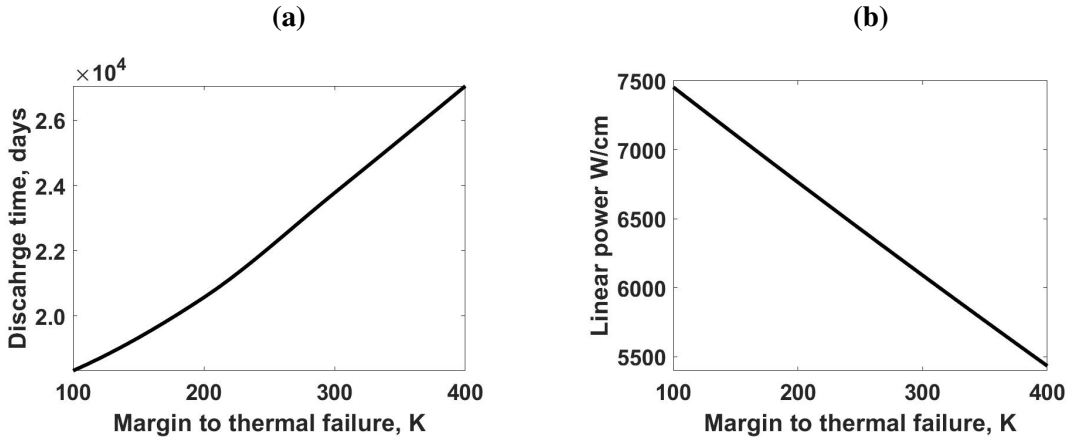

Figure 3.7. The Discharge Time(a) and Linear Power(b) for uranium nitride fuel core at an outer temperature 1500^oC.

3.5 Conclusions of the Preliminary Design

This initial study focused on (1) introducing the pre-conceptual design of the high temperature, ultra-small modular reactor, and (2) carrying out a preliminary sampling of its design space through a coupled neutronic-thermal analysis. Through this analysis, as is best presented in Section 3.3, we have laid out a strong picture of the possible operational parameters and optimal material design choices for the core. The results of the steady-state sensitivity analysis provides support in favor of utilizing uranium carbide or uranium nitride fuels. For these fuels, it appears possible to run the core at a total power density of

approximately 1 to 2 W/cm^3, a magnitude larger than the other fuel choices, even when operating with larger safety temperature margins. While providing slightly lower power densities, utilizing uranium carbide fuels for the battery core leads to a smaller optimal design. Also, it is of particular interest that the nitrogen used in the uranium nitride fuel does not require enrichment, reducing the cost of the fuel material. Using depletion analysis, it was also possible to estimate an operational time of tens of thousands of days. The ideal uranium nitride fuel design with the addition of a small reflector, as described in Table 3.3 was selected as candidate case for ongoing study.

Table 3.3. Candidate design from the preliminary design analysis.

Parameter	Value
Fuel Material	UN
Inner Graphite Radius, cm	17.5
Fuel Radius, cm	26.5
Outer Graphite Radius, cm	33.5
Beryllium Reflector Radius, cm	34
Tungsten Filament Radius, cm	34.5
Initial Criticality for 200K Margin	1.014
One-batch life-cycle, years	60
Discharge Burnup, MWd/kgU	7.5
Power Density, W/cm3	2

CHAPTER 4
ECONOMIC ANALYSIS

4.1 Methodology

4.1.1 Top-down Differential Economics

An analysis of economic competitiveness is one of the main factors in the decision to pursue a new nuclear design. Fortunately, there are many factors to the USMR design - the rejection of a coolant system, the high electricity conversion efficiency, the long cycle length, and the simple design- that should lead to major cost savings when constructing a nuclear power plants (NPP) based around the USMR units. Further, there are also the possibility of additional revenue sources, such as selling the ultra-high temperature heat for manufacturing, and less quantifiable factors such as improved safety and compactness to include. However, for technologies that break the mold of standard manufacturing and design, as the USMR design does, it becomes nearly impossible to do the line-by-line accounting including exact material and labor needs, that is favored for economic estimates by the industry.

Instead, this economic analysis, which examines a theoretical 1000 MWe USMR NPP, is based on a top-down differential model [25]. This analysis assumes that a USMR plant and a typical pressurized water reactor (PWR)plant would share many of the same costs and that PWR economic databases can be used for estimating USMR costs, except when the designs clearly differ. This method works particularly well in this case, since it is possible to isolate the savings and costs associated with major USMR specific design features (i.e. the fuel cycle and the TPVs). For the purpose of this study, the different costs of the USMR and, by default, the PWR NPPs are organized into accounts using the Generation IV International Forum's Code of Accounts [26]. The major subdivision of accounts is

given in Table 4.1 with the further breakdown of costs given in section 4.1.2.

Table 4.1. Primary breakdown of GIF accounts.

Account Codes	Account Description
10	Capitalized Preconstruction Costs
20	Capitalized Direct Costs
30	Capitalized Indirect Services Costs
40	Capitalized Owner's Costs
50	Capitalized Supplementary Costs
60	Capitalized Financial Costs
70	Annualized O&M Cost
80	Annualized Fuel Cost
90	Annualized Financial Cost

The calculations were automated utilizing the electronic spreadsheet program, Microsoft Excel. The analysis was undertaken in two major phases: deterministic and stochastic. In the deterministic phase the economic estimates were made using set costs to obtain average and best experience estimates. The average estimate utilizes a simple average between the minimum and maximum costs for each account. The best estimate utilizes minimum costs for each account, assuming best market spot prices and great experience in constructing USMR plants.

Model Inputs

Since the USMR design is still in its infancy, these cost estimates were made using a model as independent of detailed design parameters as possible. However, many of the accounts have costs that are directly related to the size of the plant and various fuel cycle parameters, so this study employs abstracted, unit and plant wide values. Table 4.2 contains these parameters and the typical values that were assumed for each parameter, as drawn from

the candidate design in Chapter 3, and unless stated otherwise, these are the values used in each calculation.

Table 4.2. Typical design parameter inputs for economic model.

Parameter	Value
Plant Parameters	
Capacity Factor (%)	95
Energy (MW)	1000
Plant Efficiency (%)	60
Total Lifetime (yr)	60
Ramp Period (yr)	5
Construction Period (yr)	1
Fuel Purchasing Plan	Capitalized
Fuel Parameters	
Burnup (MWd/kgU)	7.5
Fuel Enrichment (%)	19.75
Total Power Density (W/cm3)	2
Fuel Material	UN

Due to the demonstrated capacity of the USMR design for decades long operation, it is possible to operate the NPP as a battery design and purchase the entirety of the needed fuel at the beginning of the plant's operation. Under this option, the fuel costs are included with the overnight capital costs and can potentially make up the largest portion of the capital costs. To help lower this initial capital costs, one could build the infrastructure for the full plant and ramp up the electricity output by buying and installing a portion of the total number of units at a time over the course of several years; it would then be possible to see major saving in the process of discounting these later purchases to current dollars. Unfortunately, this will likely lead to lower lifetime electricity production and

greater LCOE. Non-fuel related annual costs are assumed to be largely scalable with the energy output of the plant and are not adjusted. Lastly, one might imagine using the USMR concept as smaller units in some axial multi-batch arrangement that would allow for fuel to be purchased as needed for the year. This would shift the major fuel costs from a capital expense to an annualized one, which introduces savings by normalizing the fuel cost over the total electricity produced in a year rather than normalizing the costs to a discounted total energy as is done in the capital case.

Stochastic Approach

In the stochastic phase, a normal cost distribution was assumed for each account, with the minimum and peak taken to be the 2 σ values. A description of the USMR design space for UN fuel that related burnup to a given total power density and fuel enrichment, without factoring core dimensionality was developed. Starting with a selection of cases from the study that will presented in chapter 5, Figure 4.1 was developed . Taking a second order polynomial fit of the data, a relationship between these burnup, power density and enrichment was described by Equation 4.1. Knowing that the burnup had to be greater than 0, and setting that the enrichment had to be relatively low, an approximation of the maximum power density for a given enrichment was developed,as shown by Equation 4.2. The USMR design space was defined by the range of enrichment from 8 to 20% and power density from 0 to the maximum power given by Equation 4.2. A uniform distribution was assumed across the design space.

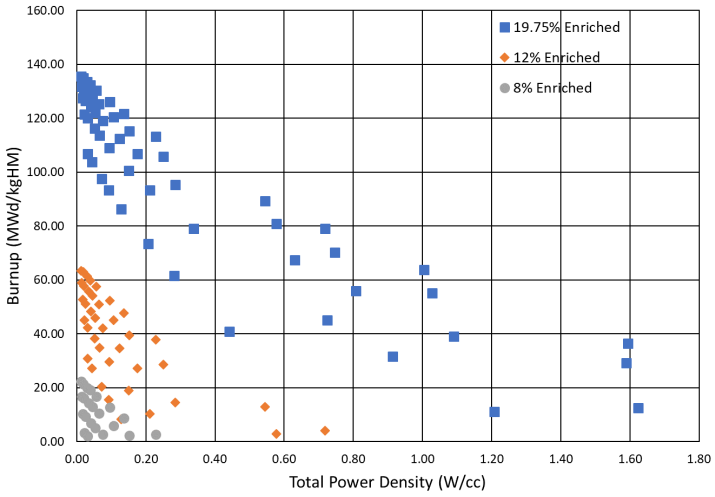

Figure 4.1. Discharge burnup as a function of enrichment and power density.

$$B = -37.59 - 69.49 * P + 5.595 * E + 34.01 * P^2 - 2.393 * P * E + 0.1405 * E^2 \quad (4.1)$$

$$P_{max} \approx 1.022 + 0.0352 * E - \sqrt{2.15 - 0.093 * E} \quad (4.2)$$

In developing the stochastic distributions for LCOE, Capital and Operating Cost, 5000 calculations were made using randomly selected enrichment and power density inputs, which was used in a derived burnup input, and cost factors for each account to use in calculating the estimates. This stochastic analysis was conducted for the four fuel cycle purchasing options: purchasing all the necessary fuel at the beginning of operation, ramping up the energy production across 5 years of fuel purchases, ramping up the energy production across 10 years of fuel purchases, and using a batch loading system to annually purchase the fuel needed to operate.

4.1.2 Description of Accounts

10-Capitalized Pre-Construction Costs

For the economic analysis, capitalized pre-construction and other capital costs were treated as overnight costs, assuming that the total costs are sunk at the beginning of the plant life in present value dollars. The pre-construction cost category, found in Table 4.3, includes costs associated with purchasing the land and acquiring the necessary permits to begin construction on the NPP. The major boon for the USMR design, in this case, is its inherent safety as a low power, solid state design. Where the typical reactor plant includes a 10-mile exclusionary zone to protect the public in the case of accidents vaporizing radiological materials, for the purposes of this analysis, it is assumed that the USMR will only require a 1-mile exclusionary radius. Further, without need for a feed water source, the proposed plant could be built on the cheapest land available. The land costs for the USMR were found using data on the cost of unirrigated, pasture land per acre and the area needed for the 1-mile exclusionary zone [27]. However, it is more difficult to determine how the permitting and license costs would change, and as such, those costs are estimated using the set values for a PWR system [28]

Table 4.3. Capitalized Pre-Construction Costs.

Code	Cost Description	Factor	Min Value ($2017/factor)	Peak Value ($2017/factor)
11	Land and Land Rights	Acreage	650	2158
		Exclusion Zone Radius (mile)	–	
12,13, & 14	Site Permits and Combined License	Unit	60000000	60000000
15	Plant Studies and Reports	Unit	8000000	8000000
19	Contingency on Pre-Construction Costs	Other Pre-construction Cost	0	0.05

20-Capitalized Direct Construction Costs

The capitalized direct costs, given in Table 4.4 include the major material, equipment and costs for the construction of the plant. This category is subdivided into line-items for specific plant buildings and systems to highlight the cost savings of the battery design. This is the largest source of capital costs for the plant and the largest source of savings from the USMR design. The prices shown in Table 4.4 were drawn from the DOE's energy economic database (EEDB) for PWRs and are scaled to the electric output of the plant [3]. The minimum costs represent PWR construction costs when constructed by the most experienced firms while the peak costs represent the construction costs incurred by a starting firm. A significant portion of the accounts are associated with the coolant loops and turbine equipment; since these structures are not required in the USMR model, those accounts are neglected in the cost estimations. Further, in the reactor island account, the

costs are scaled to twice the volume of needed units as calculated from the USMR output and power density as compared to the typical containment structure in order to factor in the potential need for a larger containment building for the low power density system [29].

[H]

Table 4.4. Capitalized Direct Construction Costs.

Code	Cost Description	Factor	Min Value ($2017/factor)	Peak Value ($2017/factor)
21	Structures and Improvements	–	–	–
211	Site Preparation/Yard Work	size (kW)	47.85	63.89
212	Reactor Island Civil Structures	size (kW)	129.71	199.34
		Core Volume	–	–
213	Turbine Generator Building	Not Necessary	44.96	73.72
214	Security Building and Gate-house	size (kW)	2.42	3.49
215	Reactor Service (Auxiliary) Building	size (kW)	33.74	51.17
216	Radwaste Building	size (kW)	27.51	43.38
217	Fuel Service Building	size (kW)	18.93	25.36
218A	Control Building	size (kW)	34.11	58.88
218B	Administration + O&M Build-ing	size (kW)	12.69	19.67
218E	Steam Generator Storage Building	Not Necessary	331.36	348.80
218K	Pipe Tunnels	Not Necessary	0.75	0.94
218L	Electrical Tunnels	size (kW)	0.13	0.17
218N	Maintenance Shop	size (kW)	1.29	1.65

218S	Wastewater Treatment Building	size (kW)	1.48	1.76
22	Reactor Equipment	–	–	–
221	Reactor Equipment	size (kW)	20.66	21.83
222	Main Heat Transport System	Not Necessary	1.93	39.73
223	Safety Systems	size (kW)	25.50	48.64
224	Radioactive Waste Processing Systems	size (kW)	40.85	59.98
225	Fuel Handling Systems	size (kW)	6.20	8.28
226	Other Reactor Plant Equipment	size (kW)	73.42	130.45
227	Reactor Instrumentation and Control (I&C)	size (kW)	41.36	45.25
228	Reactor Plant Miscellaneous Items	size (kW)	14.59	17.82
23	Turbine Generator Equipment	–	–	–
231	Turbine Generator(s)	Not Necessary	256.62	263.83
233	Condensing Systems	Not Necessary	49.77	67.64
234	Feed Heating Systems	Not Necessary	45.60	63.19
235	Other Turbine Plant Equipment	Not Necessary	42.78	76.55
236	Instrumentation and Control (I&C)	Not Necessary	13.14	15.29
237	Turbine Plant Miscellaneous Items	Not Necessary	15.81	18.56
24	Electrical Equipment	–	–	–

241	Switchgear	size (kW)	22.14	23.30
242	Station Service Equipment	size (kW)	36.96	37.19
243	Switchboards	size (kW)	3.98	4.07
244	Protective Systems Equipment	size (kW)	8.21	9.57
245	Electrical Raceway Systems	size (kW)	42.82	89.42
246	Power and Control Cables and Wiring	size (kW)	39.90	62.23
25	Heat Rejection System	–	–	–
251	Structures	Not Necessary	19.09	26.51
252	Mechanical Equipment	Not Necessary	85.19	97.72
26	Miscellaneous Equipment	–	–	–
261	Transportation and Lift Equipment	size (kW)	11.65	12.35
262	Air, Water, Plant Fuel Oil, and Steam Systems	size (kW)	53.12	93.96
263	Communications Equipment	size (kW)	12.38	14.02
264	Furnishing and Fixtures	size (kW)	5.30	5.62
29	Contingency on Direct Costs	size (kW)	0.00	0.05

30-Capitalized indirect Construction Costs

The capitalized indirect construction costs, given in Table 4.5, includes the costs associated with the design and supervision of plant construction along with the start-up commissioning costs. The price data used in these accounts was also taken from the EEDB data for a reference PWR[3]. Again, these values are scaled to the size of the NPP. It is worth noting that due to the simplicity of the USMR core and balance of plant, the final construction service costs of the USMR design will likely be lower than the PWR.

Table 4.5. Capitalized Indirect Construction Costs.

Code	Cost Description	Factor	Min Value ($2017/factor)	Peak Value ($2017/factor)
31	Field Indirect Costs	Size (kW)	411.63	755.06
32	Construction Supervision	Size (kW)	14.98	704.47
33	Commissioning and Startup Costs	Size (kW)	21.17	33.28
35	Design Services Offsite	Size (kW)	376.63	871.49
36	PM/CM Services Offsite	Size (kW)	22.26	42.12
37	Design Services Onsite	Size (kW)	23.10	37.73
38	PM/CM Services Onsite	Size (kW)	15.62	59.86
39	Contingency on Indirect Services Cost	Other Costs	0.00	0.05

40-Capitalized Owner's Costs

The capitalized owner's costs, given in Table 4.6, include the costs to hire, relocate, house, and train the employees in charge of the day to day operations once the plant starts up. These accounts primarily hinge on the number of employees, their positions and their salaries, which are further expanded in Table 4.7 [30]. In a traditional PWR, the plant operations can be divided into two main categories, neutronics and thermal-hydraulic systems. Without the thermal-hydraulic system, it is assumed that the USMR plant would employ only half the number of employees in each category as compared to the reference PWR plant, as given in Table 4.7. The staff salary is scaled with the construction period to give an estimate for the cost to retain the staff needed at the plant ahead of startup. The staff housing costs are based on standard relocation packages scaled by the number of employees [31]. Lastly, the salary related costs include the estimate for the payroll taxes on

the salaries paid to retain the NPP staff [32].

Table 4.6. Capitalized Owner's Costs.

Code	Cost Description	Factor	Min Value ($2017/factor)	Peak Value ($2017/factor)
41	Staff Recruitment and Training	Construction Period	30380710	40986715.1
42	Staff Housing	Number of Staff	20000	65000
43	Staff Salary-Related Costs	Salary Costs	0.05	0.15
49	Contingency on Owner's Costs	Other Costs	0	0.05

[H]

Table 4.7. Plant Staff Breakdown and Annual Salary.

Cost Description	Staff Employed	Min Salary ($2017)	Peak Salary ($2017)
Admin Office			
Plant Manager	1	216828	290511.6
Assistant manager	1	150945.2	203358.1
Public relations	1	95897.53	127825.1
Environmental control	1	95897.53	127825.1
Training	24	104864.6	142350.7
Safety and fire protection engineering	4	88923.16	119109.7
Administrative services	40	57538.52	78438.12
Security	63	51809.57	69722.78

Health	2	57538.52	77605.31
Operations			
Supervision	2	111340.8	148160.9
Shift operations	52	93406.68	124920
Engineering	10	93406.68	136540.4
Maintenance			
Supervision	4	103245.5	139445.6
Crafts	70	73355.38	98773.93
Annualized peak maintenance	28	73355.38	98773.93
Diagnostic Engineering	6	93406.68	127825.1
Quality control	4	79333.41	107489.3
Storekeepers	5	67626.44	90058.58
Grounds	2	52307.74	70550.28
Technical Support			
Reactor engineering	3	111340.8	148160.9
Radiochem and water chem	6	103245.5	139445.6
Engineering	15	95274.81	127825.1
Technicians	30	77465.27	104584.2
Health physics	18	79707.03	104584.2
Licensing Assurance	2	95274.81	128502.3

50-Capitalized Supplementary Costs

The capitalized supplementary costs, shown in Table 4.8, are costs, unrelated to plant construction that are incurred prior to plant start-up. This category including the total

property and sales taxes, spare parts, insurance, decommissioning and importantly, initial fuel costs. The costs associated with accounts 51, 52 ,53, and 54 are included in the EEDB account used for the price data for account 31. The decommissioning costs data use in this analysis comes from the Nuclear Energy Agencies decommissioning estimates [33]. The most important factor in this category, as suggested previously, is the costs for the initial fuel loading, which are given as "A" and "B" in Table 4.8 since they are dependent on fuel cycle and operational parameters. The fuel costs are further broken down in Table 4.9.

Table 4.8. Capitalized Supplementary Costs.

Code	Cost Description	Factor	Min Value ($2017/factor)	Peak Value ($2017/factor)
51	Shipping and Transportation Costs	–		
52	Spare Parts	–		
53	Taxes	–		
54	Insurance	–		
55	Initial Fuel Core Load	Unit	A	B
58	Decommissioning Costs	Unit	1.50E+08	4.70E+08
59	Contingency on Supplementary Costs	Others	0	0.05

For the purpose of this study, the cost of the initial core loading is estimated based on the amounts and prices of the materials needed, the cost to manufacture the fuel elements and the cost of structural materials which are derived from an experimental relation. The initial core is so costly due to two factors: the high enrichment of the fuel that is carried over from initial design analysis and the large amount of fuel needed to operate the cores continuously through the plant life-cycle.

Starting with the fuel utilization, the energy output, and the life cycle of the plant, the

mass of the fuel consumed by the plant can be simply derived. From there, the cost for enriching the fuel as well as the bulk quantity of uranium needed per kilogram of fuel can be found using the standard separative work (SWU) equations, Equation 4.3 and 4.4. Here, "T", "P", and "F" represent the masses of uranium leaving the enrichment process as waste (tails), leaving the process as enriched fuel (products), and entering the process as bulk uranium (feeds), respectively. The enrichments of the tails, product and feed streams are given as "t", "p", and "f".

$$SWU = P\,(1-2p)\,ln\left(\frac{1-p}{p}\right) + T\,(1-2t)\,ln\left(\frac{1-t}{t}\right) - F\,(1-2f)\,ln\left(\frac{1-f}{f}\right) \tag{4.3}$$

$$\frac{T}{P} = \frac{p-f}{f-t},\ \frac{F}{P} = \frac{p-t}{f-t} \tag{4.4}$$

The cost of the fuel element can be explicitly given in Equation 4.5, where "i" denotes other elements present in the fuel molecule. As is suggested by the structure of Equation 4.5, there is an ideal tails enrichment that minimizes the combined cost of the fuel enrichment process and fuel material. By setting the derivative of the fuel cost by tails enrichment to zero and substituting the definitions given in Equation 4.4 and dividing out known terms, Equation 4.6 can be found. Through simplification, the ideal tails enrichment can be found as function of feed enrichment, bulk uranium costs, and enrichment costs, as given in Equation 4.4.

$$C_{Fuel} = C_{SWU} * SWU + C_U * F + \Sigma C_i * M_I * \frac{mol_i}{mol_U} * \frac{P}{M_U} + C_{Man.} \tag{4.5}$$

$$\frac{dC_{Fuel}}{dt} = 0 \approx C_{SWU}\left[\frac{d}{dt}\left(\frac{p-f}{f-t}\frac{(1-2t)^2}{t}\right) - \frac{d}{dt}\left(\frac{p-t}{f-t}\frac{(1-2f)^2}{f}\right)\right] + C_{Fuel}\frac{d}{dt}\left(\frac{p-t}{f-t}\right) \tag{4.6}$$

$$t = \frac{f - f\sqrt{2 - \frac{C_U}{C_{SWU}}f}}{\frac{C_U}{C_{SWU}}f - 1} \tag{4.7}$$

For full picture of the cost of the USMR core, it is necessary to take into account the structural costs of the fuel assemblies, which is heavily dependent on the amount moderation for each design case. This moderation level also directly affects the total power density. For each of the cases described in the design analyses in chapters 3 and 5, the ratio of the structural material to fuel costs were calculated according to Equation 4.8, using the radii as defined in Figure 4.2 and the costs and densities of graphite, uranium nitride, beryllium oxide [34] and tungsten[35].

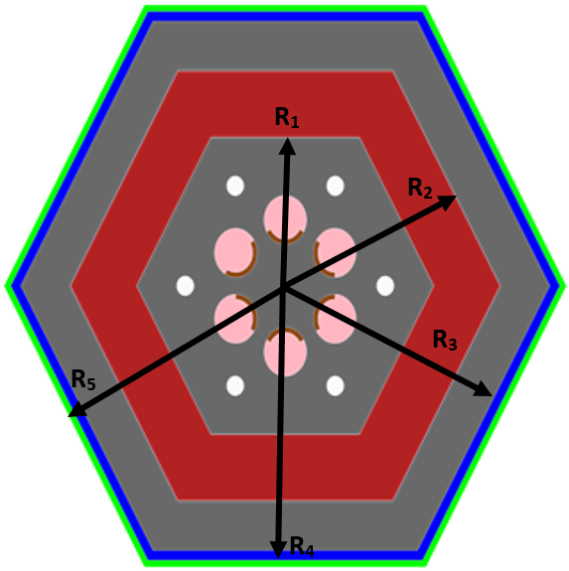

Figure 4.2. The hexagonal cross-section with labeled radii for use in Equation 4.8.

$$\frac{C_{Str}}{C_{Fuel}} = \frac{\frac{3\sqrt{3}}{2}\left(C\rho_{Graph}\left(R_1^2 + R_3^2 - R_2^2\right) + C\rho_{Be}\left(R_4^2 - R_3^2\right) + C\rho_{W}\left(R_5^2 - R_4^2\right)\right)}{\frac{3\sqrt{3}}{2}C\rho_{UN}\left(R_2^2 - R_1^2\right)} \tag{4.8}$$

The relationship between structural material cost ratio, power density and enrichment is laid out in Figure 4.3 and Equation 4.9. In Equation 4.9 "A" is a constant coefficient defined by the fit, "a" is the enrichment scaling factor, and "b" is the power density scaling factor, defined by the ranges in rows 18, 19, and 20 of Table 4.9, respectively.

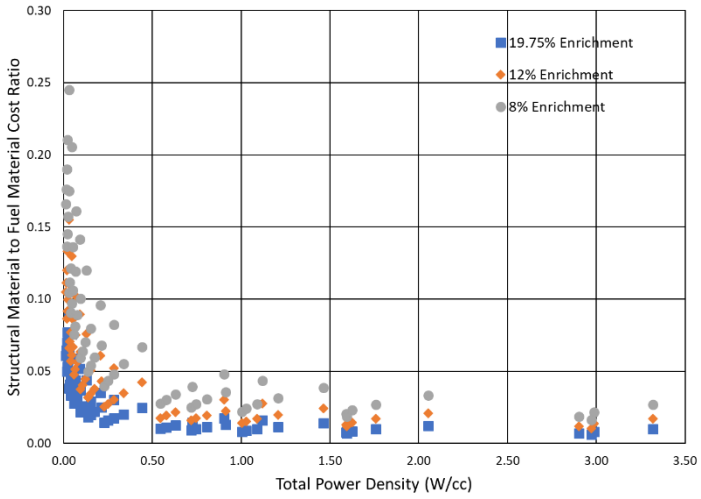

Figure 4.3. The ratio of the structural material to fuel material cost as a function of power density.

$$\frac{C_{Str.}}{C_{Fuel}} = A\left(Enrichment\,[\%]\right)^{-a}\left(PowerDensity\left[W/cm^3\right]\right)^{-b} \tag{4.9}$$

[H]

Table 4.9. USMR unit core costs.

Cost Description	Factor	Min Value ($2017/factor)	Peak Value ($2017/factor)	Source

Uranium Bulk Costs	Nat Uranium Needed	44.0528634	47.35683	[36]
	P enrichment	–		
	F Enrichment	–		
	T Enrich-ment	–		
	Enr Uranium (UC)	–		
	Enr Uranium (UN)	–		
	Fuel Needed (kg)	–		
Conversion Costs	Nat Uranium Needed (kg)	11	13	[37]
Hydrogen Bulk Costs	Hydrogen Needed (kg)	5	10	[38]
	molH/UN	–		
Nitrogen Bulk Costs	Nitrogen Needed (kg)	0.0485	0.242	[39]
	molN/UN	–		
Carbon Bulk Costs	Carbon Needed (kg)	0.85	2	[40]
	molC/UC	–		
Enrichment Cost	SWU	60	160	[41]
Manufacturing	Fuel Needed (kg)	244.1	330.26	[37]

Cost of Structural Materials	Fuel Element Cost	0.229	0.484	
	Enrichment	0.969	1.264	
	Power Density	0.364	0.442	

60-Capitalized Financial Costs

The capitalized financial costs, given in Table 4.10, includes accounts related to the changing value of money, fees and loan interest incurred during the construction of the NPP. Account 61 is usually neglected when conducting economic analysis in terms of fixed year costs, as this analysis does. It is assumed for this analysis that the initial fees are already included in the combined license under which the NPP would operate. Lastly, during plant operation, it can be assumed that the plant costs, even capitalized ones are entirely covered through the sale of electricity at the LCOE or above. However, during construction, the costs of the plant have to be financed, and account 63 includes the interest accrued an the cost of the first three major accounts across the construction period, given an arbitrary range of interest rates.

Table 4.10. Capitalized Financial Costs.

Code	Cost Description	Factor	Min Value ($2017/factor)	Peak Value ($2017/factor)
61	Escalation	–		
62	Fees	–		
63	Interest During Construction	Accounts 10/20/30	0.025	0.075
		Construction Period, Years	–	
69	Contingency on Financial Costs	Other	0	0.05

70-Annualized Operating and Maintenance Costs

The annualized operating and maintenance costs, given in Table 4.11, are the annual cost associated with employing staff and replacing the maintenance supplies over the year. The costs related to the staff are drawn from Table 4.7 and the material costs are pulled from the DOE's cost estimating guidelines for NPP operation [30]. A significant portion of the annual costs is based on the annual replacement of TPV panels after exposure to the mixed gamma and neutron fields leads to damage and a degrading of total system efficiency. Depending on field strength and the acceptable loss of efficiency, it has been estimated that these panels would have to be replaced every two to five years which is used in deriving the annual costs of the TPVs [8]. The annual cost of these replacements per watt of electrical output, laid out in Figure 4.4, is based on the temperature of the outer surface, which determines the system efficiency, and the rate of TPV replacement.

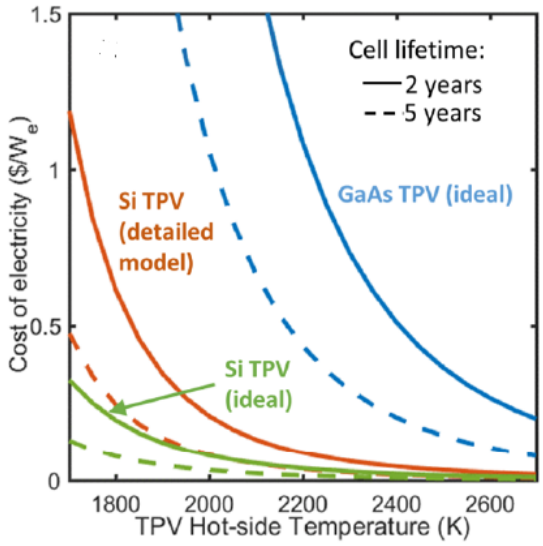

Figure 4.4. The annual cost of TPV replacement per watt of electric output (We) dependent on surface temperature of emitter and TPV replacement rate.

Table 4.11. Annualized O&M Costs.

Code	Cost Description	Factor	Min Value	Peak Value
71,72	Staff Salary	Salary	30380710	40986715
73	Salary-Related Costs	Salary Costs	0.05	0.15
74,75	Operating Chemicals and Lubricants	Size(kW)	7.134545	8.72
75B	TPV	Size (W)	0.1	0.4
76	Utilities, Supplies, and Consumables	Size(kW)	13.37727	16.35
78	Taxes and Insurance	Size(kW)	7.294615	10.56462
79	Contingency on Annualized O&M Costs	Other	0	0.05

80-Annualized Fuel Costs

The annualized fuel costs, given in Table 4.12, is the cost to add fresh USMR units to the plant each year to replace spent ones and includes the costs of the fuel material itself and the operational costs associated with refueling. When not specifically considering an annualized fuel scheme, this category is not used in calculating the USMR cost estimates. When included, the fuel costs are derived from the data in Table 4.9 and the refueling and reprocessing costs are drawn from the Generation IV international forum's proceedings [42]. Like in Table 4.8, "A" and "B" are dependent on the fuel cycle and operational parameters.

Table 4.12. Annualized Fuel Costs.

Code	Cost Description	Factor	Min Value	Peak Value
81, 86,87	Refueling and Reprocessing Operations	Annual Energy (MWhr)	1	3.75
84	Nuclear Fuel	Unit	A	B
89	Contingency on Annualized Fuel Costs	Other Costs ($)	0	0.05

90-Annualized Financial Costs

The annualized financial costs, given in Table 4.13, includes the annual fees for operating the plant and the annual adjustments in the value and the opportunity cost of the dollar. Since this analysis uses fixed dollar prices, the escalation can be neglected. Further, under the assumption that the money is appropriated specifically to be used for operations of the plant, the cost of money is neglected. This leaves only the financial costs of the annual license which is set by the NRC per reactor [43]. For the purpose of this study, it is assumed for ease that the license fee is applied to the whole 1000 MWe, multi-unit site rather than per unit, since this is the typical scale of reactors the currently fall under the licensing rule.

Table 4.13. Annualized Financial Costs.

Code	Cost Description	Factor	Min Value ($2017/factor)	Peak Value ($2017/factor)
91	Escalation	–		
92	Fees	Unit	4308000	4308000
93	Cost of Money	–		
99	Contingency on Annualized Financial Costs	–		

4.1.3 Learning Rate and Scaling Law Sampling

In addition to the top-down differential economic analysis, the effect of various power scaling coefficients and learning rates on the ability for a small modular reactor, specifically the USMR, to break even with larger reactors was examined. Of particular concern to this examination was the determination of the amount of SMR units in terms of additional electric generating capacity would be needed for the gains in learning to break-even with the losses in size of the plant. In order to provide a total probability for the USMR at a 1 and 10 MWe size to be able to break-even with a 1000 MWe plant with the addition of a reasonable capacity of USMR plants (30MWe), using Equation 1.4 in section 1.4.2, the break-even capacities were calculated for 10,000 uniform samplings of the power scaling factor in Table 4.14 and learning rates in Table 4.15. The power scaling factors in Table 4.14 are drawn from a review of nuclear industry power scaling studies [13]. Because the USMR is such a novel design, the learning rates in Table 4.15 are drawn from surveys across the energy sector [44].

Table 4.14. Results of nuclear power scaling (a) surveys.

Year of Survey	Scale	Note on Source	Year of Survey	Scale	Note on Source
1968	-0.25	LWR Total Cost	1979	0	LWR Regression of Historic Data
1968	-0.49	Total Cost	1978	-0.55	Direct and Indirect Costs
1969	-0.36	Total Cost	1979	-0.6	PWR Direct and Indirect Costs
1971	-0.32	Total Cost	1979	-0.76	LWR Direct and Indirect Costs
1973	-0.6	LWR Direct Cost	1979	-0.51	Total Cost
1975	-0.53	BWR Total Cost	1980	-0.41	Total Cost
1976	-0.54	LWR Total Costs	1980	-0.75	Direct and Indirect Costs
1976	-0.29	Direct and Indirect Costs	1981	-0.2	Regression of Historic Data
1977	-0.14	LWR Total Costs	1981	-0.6	Direct Cost
1977	-0.24	LWR Total Costs	1982	-0.37	Regression of Historic Data
1978	-0.2	LWR Regression of Historic Data	1982	-0.47	LWR Direct and Indirect Costs
1978	-0.5	LWR Regression of Historic Data	1982	-0.37	LWR Engineering Cost Estimates
1978	-0.3	LWR Regression of Historic Data	1982	-0.51	Regression of Historic Data

Table 4.15. Results energy source learning rate survey.

Source	LR	Source	LR	Source	LC
NPP	0.058	Hydro	0.014	Coal	0.076
Lignite	0.086	GTCC	0.34	GTCC	0.26
Wind	0.17	Wind	0.18	Wind	0.08
Wind	0.08	Solar	0.2	Ethanol	0.22

4.2 Results

4.2.1 Deterministic Results

The best and average LCOE estimate as compared to data on reference electricity sources provided by the U.S. Energy Information Agency is presented in Figure 4.5 [45]. In this figure, the default case in Table 4.2 with a capitalized fuel purchase plan and an annual fuel purchase plan are presented with both average and best estimates. Further, the LCOE is broken into capital costs and fixed operating costs, variable operating costs in the form of fuel costs, and the USMR specific cost to replace the TPVs. It is quickly evident that the decision to optimize the USMR design for compactness and high power density does not lead to an economically desirable design for a capitalized fuel purchase plan and is only economically competitive with the annual fuel plan under the most optimistic estimates. Compared to the reference power sources, fuel costs for this iteration of the USMR design are a much more significant portion of the total costs, likely, due to its very poor fuel utilization.

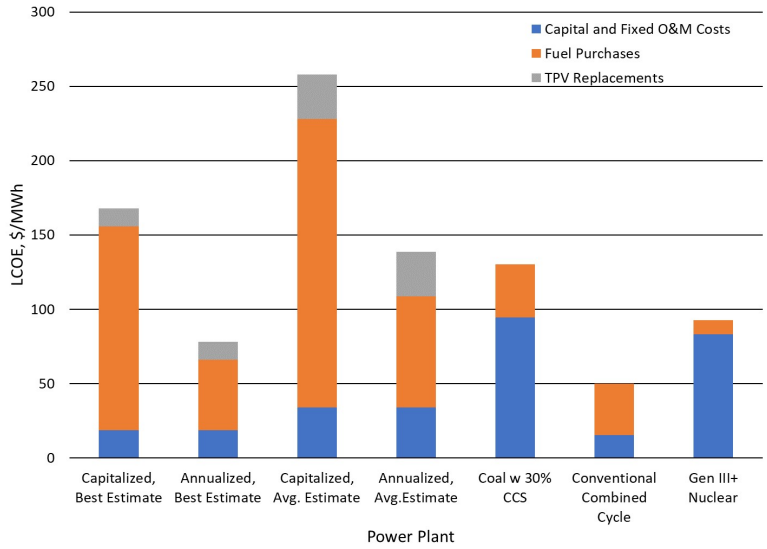

Figure 4.5. Comparison of the USMR best and average LCOE estimates to various power sources and the breakdown of LCOE costs for USMR based on fuel purchase plan.

Figure 4.6 presents a mapping of the average and best estimates in the capital and operating cost space, for the default design under all four fuel purchasing plans. The separate clustering of the reference sources highlight the three potential operating regimes for the USMR: baseload, mid-merit, and peak load. Again, it is trivial to see that the estimates USMR design iteration from Table 4.2 are, for the most part, too high in both operating and capital cost to find an economically viable niche. Only under the best conditions might the design with annual fuel purchase find a viable market among peak-load plants.

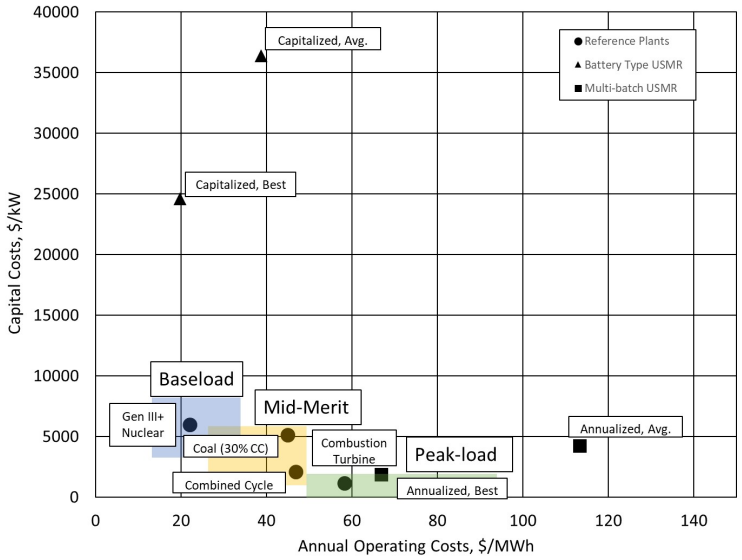

Figure 4.6. Comparison between the USMR best and average capital and operating cost estimates for various fuel purchasing plans and typical capital and operating cost of various power sources.

4.2.2 Stochastic Results

As a means to examine the uncertainty in the price for each account and the final design, 5000 calculations, based on a random sampling of the account prices and design space, were conducted using the default input parameters in Table 4.2 for four fuel purchase plans: capitalized with no ramp period, capitalized with a five-year ramp, capitalized with a ten-year ramp and annualized. Figure 4.7 shows the LCOE probability curves for the four fuel purchase options along with the LCOE of the reference PWR NPP. Figure 4.8 includes a mapping of the capital and annual costs for each calculation, and Table 4.16 includes the averages and standard deviations of the LCOE, capital costs and annual operating and maintenance cost for the four fuel purchasing plans. What is clear from these figures and tables is that there is a high probability of producing a USMR plant with lower LCOE than typical Gen III+ NPP and with a capital cost less than $7000/kW. It is important to note that the stochastic study only shows the USMR as being potentially viable after the limitation of the design to the candidate, presented in Table 4.2, has been dropped.

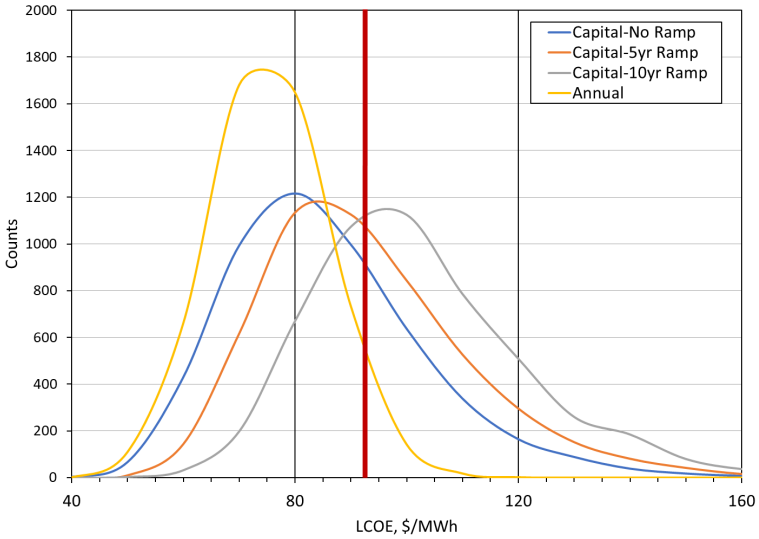

Figure 4.7. LCOE Probability Curves from 5000 runs of each fuel cycle design using stochastic evaluation of the USMR costs with LCOE of Gen III+ reactors ($93/MWh) depicted.

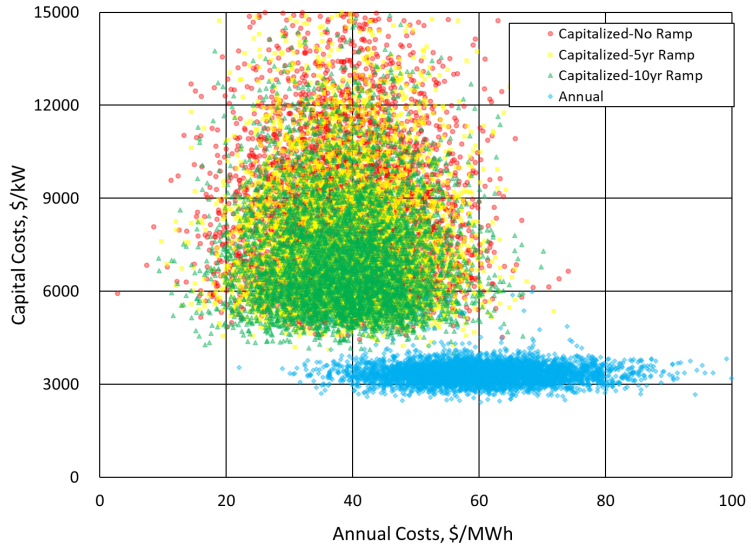

Figure 4.8. Distribution of Capital and Annual Costs from 5000 runs of each fuel cycle design using stochastic evaluation of the USMR costs.

Table 4.16. Summary of stochastic sampling.

Purchase Plan	Average LCOE ($ 2017 /MWh)	1σ	Avg. Capital Costs ($ 2017 /kW)	1σ	Avg. Annual Costs ($ 2017/MWh)	1σ
Capitalized, No Ramp	90.44	17.75	8570	2525	38.82	9.07
Capitalized, 5 yr Ramp	97.82	18.54	7769	2153	39.00	8.80
Capitalized, 10 yr Ramp	107.18	19.62	7185	1848	38.68	9.06
Annualized	80.42	10.41	3351	302	60.24	10.26

4.2.3 Economic Sensitivities

In order to guide the ongoing design efforts, especially in light of the large estimates calculated for the first converged solution, it is valuable to show the effect of different plant and core design parameters on the final cost of electricity and to enumerate those factors based on their importance. Figures 4.9 through 4.17 each present the effect of varying one of the inputs listed in Table 4.2 on the final LCOE estimates for both average and best estimates while maintaining the other parameters. The results presented here are only based on the capitalized fuel plans and are largely predictable for those cases. At a core level, lowering enrichment and increasing fuel utilization, conversion efficiency and power density should lower the amount of fuel required and cost. On a plant-wide level, increasing the operational capacity and the size of the plant while decreasing the construction period, ramp period and lifetime can improve the USMR economic performance. It is worth noting that the behavior of the LCOE with plant lifetime is largely an artifact of the decision to operate the USMR plant as a nuclear battery with the fuel for the lifetime purchased upfront or a

cycled plant with fuel cost spread across the lifetime. For capitalization, an increase in operational life of the core requires more overnight fuel purchase with the discounted electric power weighing less to normalization than the output from the initial years.

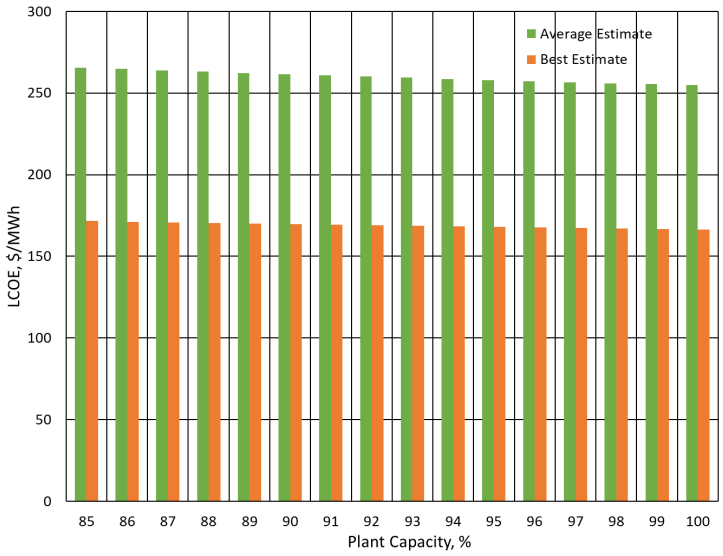

Figure 4.9. LCOE estimates as a function of plant capacity.

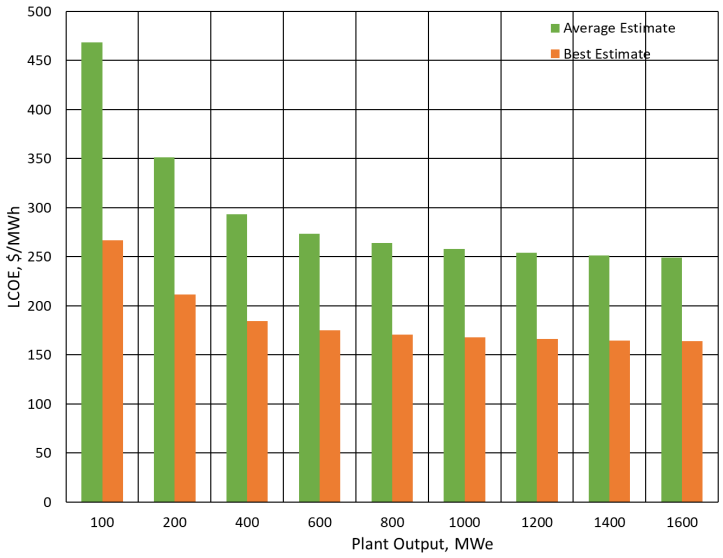

Figure 4.10. LCOE estimates as a function of plant size.

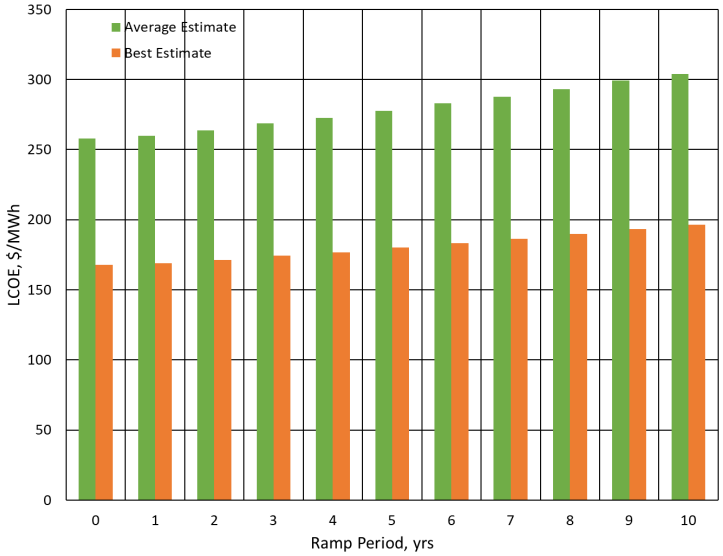

Figure 4.11. LCOE estimates as a function of interval installation period.

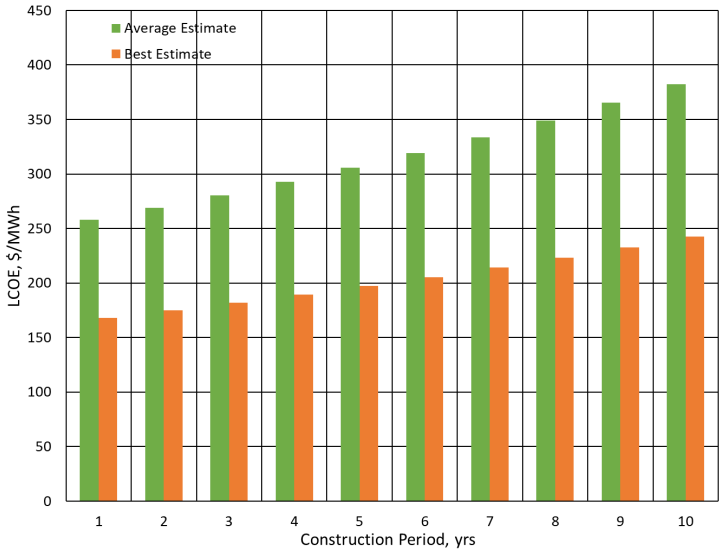

Figure 4.12. LCOE estimates as a function of construction period.

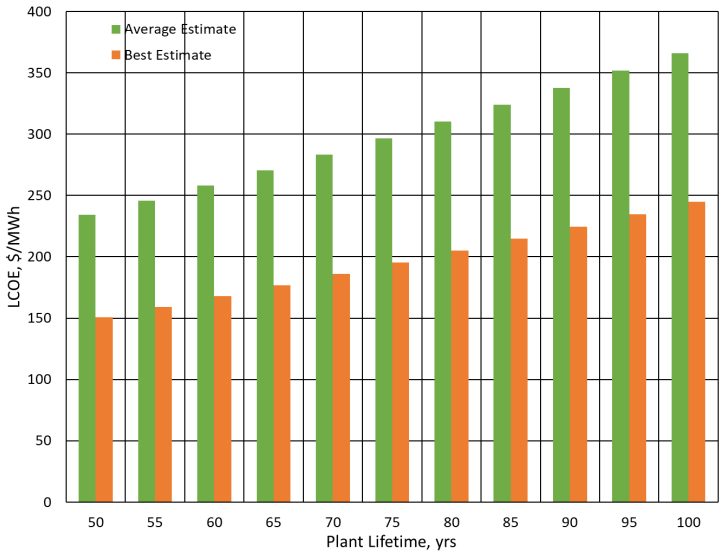

Figure 4.13. LCOE estimates as a function of plant lifetime.

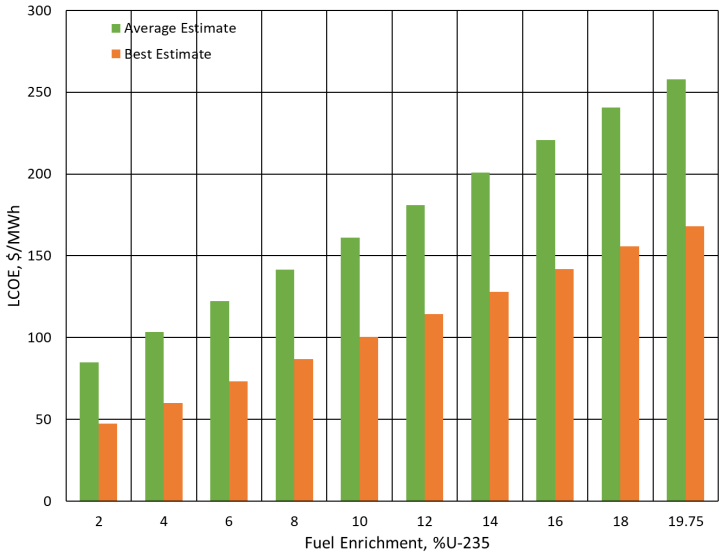

Figure 4.14. LCOE estimates as a function of fuel enrichment.

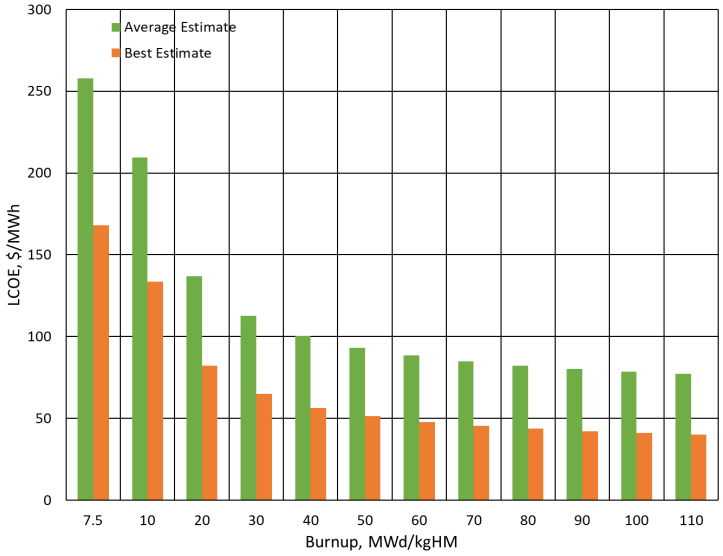

Figure 4.15. LCOE estimates as a function of fuel utilization.

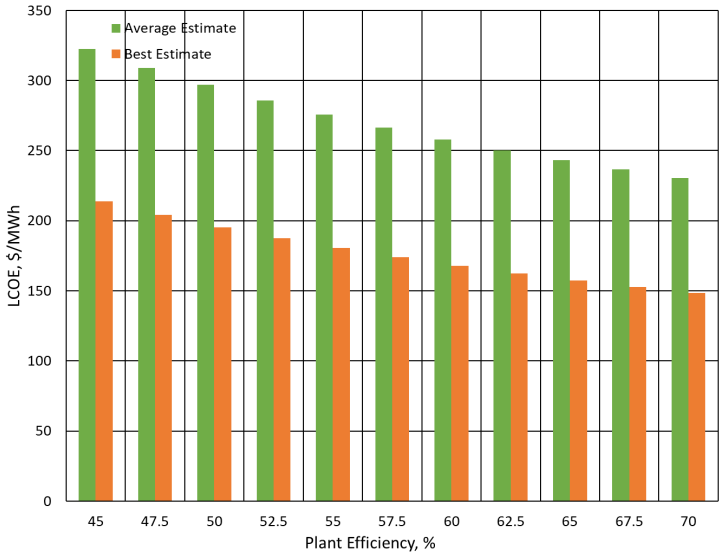

Figure 4.16. LCOE estimates as a function of conversion efficiency.

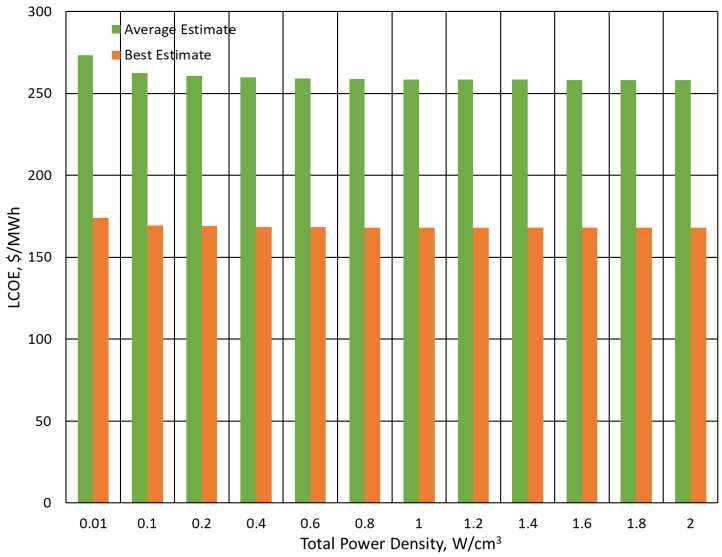

Figure 4.17. LCOE estimates as a function of total power density of the core.

Up to this point, all the cost estimates have been calculated using uranium nitride as the fuel since it was the most promising option according to the initial design study. However, uranium carbide showed only slightly worse neutronic performance, and the thermal mechanical behavior of the whole system will likely be improved when utilizing UC as a fuel option. Figure 4.18 shows a comparison of the average and best LCOE estimates when using the two fuel options while utilizing the other default inputs of Table 4.2. As is clear in the figure, the difference in the LCOE is negligible, on the order of 10s of cents. This is possible since the UN fuel studied for use with the USMR design utilizes unenriched nitrogen which is not typical to other UN fuel proposals.

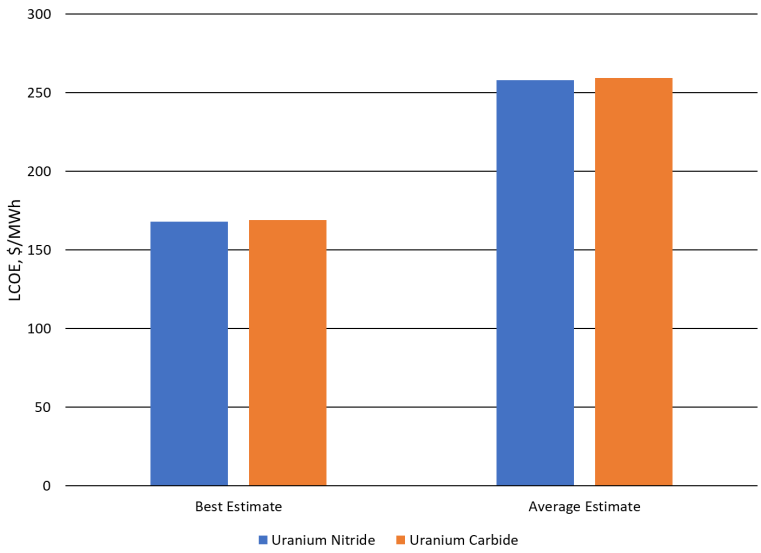

Figure 4.18. Comparison of LCOE estimates for selection of uranium nitride and uranium carbide fuel.

In order to compare the magnitude of the effects of changing design parameters, the relative differential, defined mathematically in Equation 4.10 was used as the figure of merit. The average relative differential defines the percent change in a function's value per percent change in the input across the range of variance. Table 4.17 lists these relative differentials of LCOE and capital costs for each of the parameters. It is worth noting that for plant capacity and ramp period, their impact on the capital costs is antithetical to the LCOE. This is due to the way in which these factors change the cost of the initial core, through discounting the cost or changing the amount of fuel consumed, while affecting the total energy produced by the plant.

$$Relative\ Differential = \frac{dY/Y}{dX/X} \approx \Sigma \frac{1}{N} \frac{\frac{Y_{i+1}-Y_i}{Y_i}}{\frac{X_{i+1}-X_i}{X_i}} \tag{4.10}$$

Table 4.17. LCOE and capital cost relative differentials.

Parameter	LCOE Relative Differential	Capital Costs Relative Differential
Plant Design Parameters		
Plant Lifetime	0.653	0.899
Capacity	-0.252	0.881
Construction Period	0.227	0.034
Electricity Output	-0.118	-0.111
Ramp Period	0.082	-0.116
Core Design Parameters		
Plant Efficiency	-0.731	-0.853
Enrichment	0.560	0.745
Discharge Burnup	-0.285	-0.442
Power Density	-0.004	-0.004

4.2.4 Break-even Sampling

Figure 4.19 shows the additional capacity needed to be added for a 1 and 10 MWe size plant for various power scaling and learning curves. The hope for micro-reactors is that the lower power for each unit would lead to a lower additional capacity required to be competitive. Figure 4.19 shows that this only the case for where all sized smaller reactors are viable. However, it is noteworthy that there is also a significant region of stability between 1 and 10's of GW shared by all, which suggests that the USMR smaller size is also not a detriment. Unfortunately, this leaves us with having to reasonably prove that the USMR has a lower power scaling factor and higher learning curve than an LWR based SMR. This might prove difficult to do since the primary cost of the USMR is in the material costs which typically do not have a high learning rate.

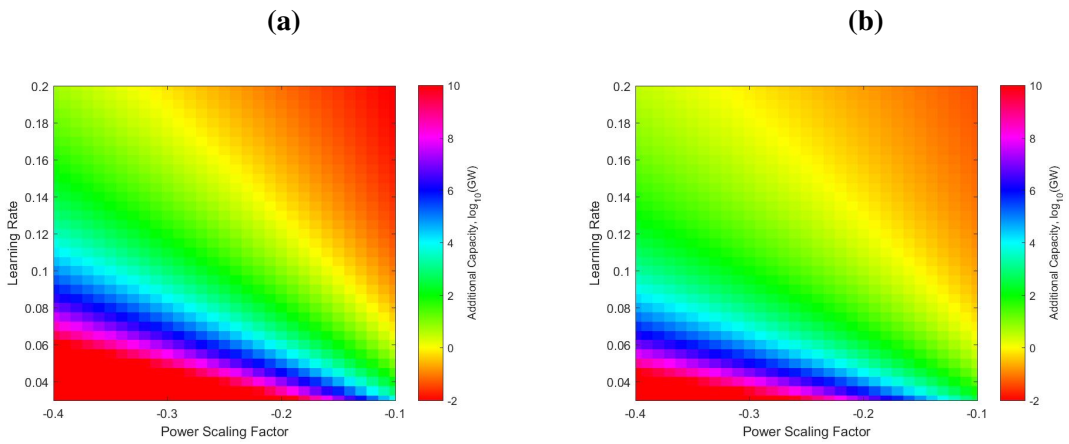

Figure 4.19. Additional capacity worth of units needed to be added to the grid in order for the break-even analysis with a 1 and 10 MWe size plant.

Figure 4.20 presents the results of performing 10,000 random sample of the power scaling factors and learning rates found in Table 4.14 and 4.15 for both a 1 MW and 10 MW plant. As can be seen in the figure, for a significant portion of the cases, both the 1 and 10 MWe would only require the construction of 10's of GW or less of additional capacity of USMR units before gains from learning rate outpaced the loss in unit size. Under the assumptions of the sampling there is a 48.4% likelihood for a 1 MWe unit design and a 57.8% likelihood for a 10 MWe unit design to balance out the law of scaling with less than 30 GW of additional capacity. This suggest that there is a realistic route for the USMR to take advantage of the law of multiples. For example, under a learning rate of 15% and power scaling of 30%, only 4.4 GWe worth of 10MWe units and 9.3 GWe worth of 1MWe, which are amounts of additional capacity that can realistically be added to the US electric grid.

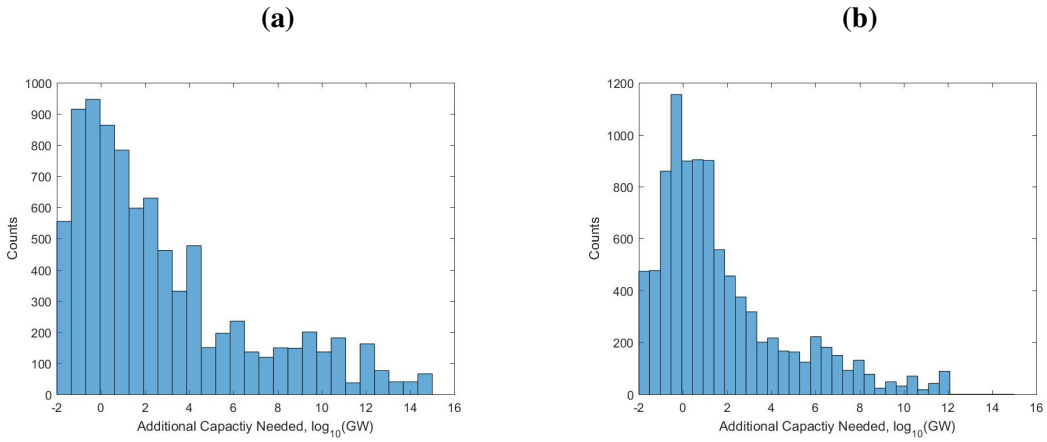

Figure 4.20. Stochastic distribution of additional capacity worth of units needed to be added to the grid for the break-even analysis with a 1 and 10 MWe size plant.

4.3 Conclusions

The deterministic economic estimates of the design brought forward from chapter 3 are hugely disappointing. However, by loosening up the design space in the stochastic, it is clear that there is a significant likelihood for a design coming out of the USMR project to be economically viable. Knowing that it is possible to make truly economically competitive designs from the USMR units adds even more significance to the takeaway messages from the economic sensitivity studies. Setting aside the plant design parameters such as size, life time, and construction plan for future work on developing the full balance of plant for various USMR NPP sizes. The four economic factors at play at this stage, in order of importance are the fuel efficiency, enrichment, burnup and power density. In terms of physical design parameters, the efficiency is directly dependent on the surface temperature; enrichment is an independent design choice but limits the minimum core size; the burnup is directly proportional to the enrichment; and the power density is inversely dependent on size of the core. Significantly, the initial assumption used in the preliminary study, that a more compact USMR core with is preferable has been disproven by the fact that the burnup, which is benefited by larger, more moderated systems, is over 75 times more impactful to the final costs.

CHAPTER 5
ECONOMICS GUIDED DESIGN

5.1 Basis

The economic guided design analysis utilized the coupled computational tool, described in Chapter 2 and was driven by the aim of improving the discharge burnup. The initial design was severely under-moderated with an initial moderating ratio, the ratio of volumes of moderating to fuel material, of 1.83. In order to address this, this study looked at three main design variables for the uranium nitride fuel: the thickness of the inner moderator, the thickness of the outer moderator, and the enrichment. The fuel region, beryllium reflector and tungsten thickness were set at 9 cm, 1 cm, and 0.5 cm, respectively. An outer surface temperature of 1300 K and an acceptable margin to material failure of 300 K were set. For the purpose of this study, the operational powers were derived from the beginning of the fuel cycle power and temperature profiles at an assumed steady-state. From these derived powers, time-dependent depletion analyses were performed on the individual cases to formulate the discharge burnup for a one-batch cycle.

5.2 Results

Figure 5.1 presents the leaked flux as a function of the moderating thickness and enrichment. As can be seen, the effect of the leaked flux is largely dependent on the thickness of the outer moderator which acts to reflect and attenuate the flux leaving the central region of the USMR unit. The leakage flux plays two key components of the USMR design. first, the impact of lost of neutrons can be hugely significant for a smaller core to be able to maintain criticality. The failure of the initial converged design with an outer moderator thickness of 7 cm in the area of fuel utilization can be largely attributed to having a leakage up to 2

orders of magnitude greater than other considered designs. Second, the amount of leaked neutron flux that would reach the TPVs is significant to the rate at which the TPVs would need replacement. Enrichment does not play a significant role here since the only other key factor to leaked flux is the power level and, therefore, rate of fissions. Figure 5.2 provides the full picture of the moderating regions and burnup. Increasing the thickness of interior graphite region also improves burnup by increasing the thermalization of neutrons crossing through the central region. Increasing the enrichment also plays a key role by allowing a lengthening of the operational length of the unit. A clearer comparison between enrichment levels is presented in Table 5.1 which shows the maximum burnup possible for 8, 12, and 19.75% enrichment for a given moderator ratio.

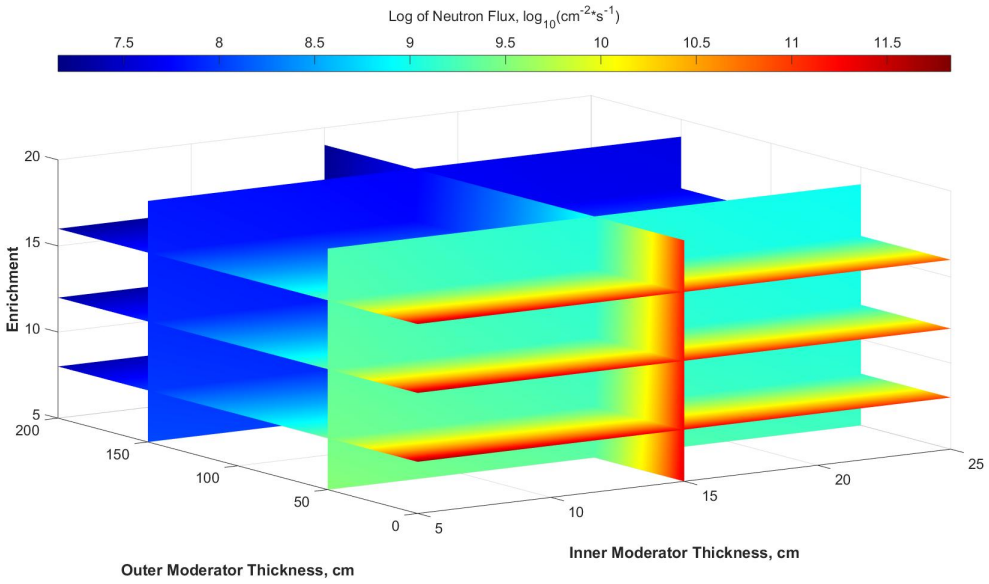

Figure 5.1. Leaked flux at exterior surface as a function of enrichment, outer moderator thickness, and inner moderator thickness.

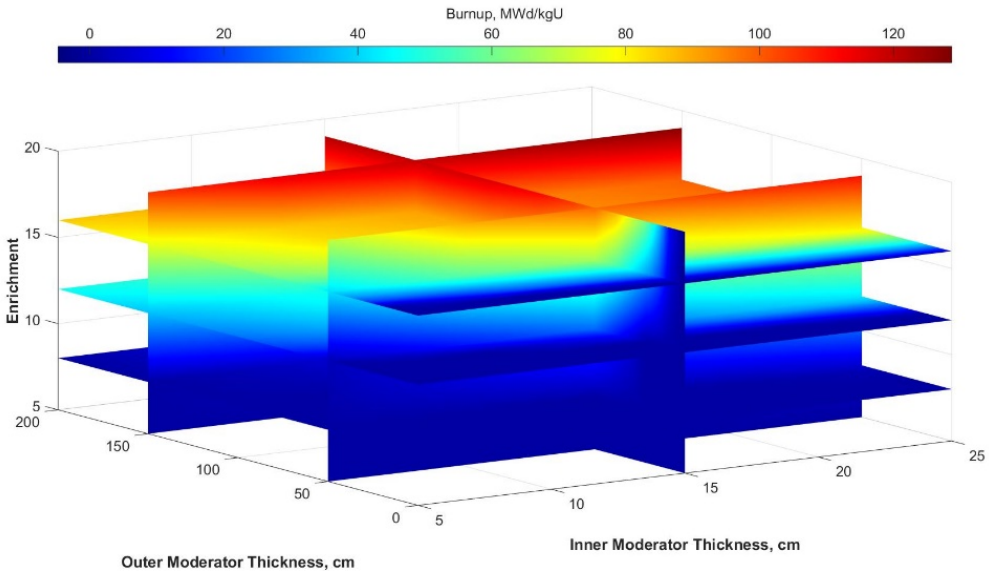

Figure 5.2. Burnup as a function of enrichment, outer moderator thickness, and inner moderator thickness.

Table 5.1. The maximum discharge burnup for each enrichment at the moderating ratios of 25 and 100.

Fuel Enrichment	Vm/Vf = 25	Vm/Vf =100
8%	15	24
12%	55	65
19.75%	130	137

The major and expected trade off for the gains in burnup can be seen in the behavior of the power density and total linear power presented in Figures 5.3 and 5.4. For a given set of outer boundary temperature and safety margin, the power is inversely proportional to the radius of the USMR design. The power density is then scaled by the volume of the unit. Due to these behaviors, the a minor change in the radius of the USMR core can lead to a major loss in power as can be seen in the figures. Fortunately, these losses level off and as was revealed in the sensitivity analysis in Chapter 4, the power density has a relatively insignificant role in the total cost compared to fuel utilization.

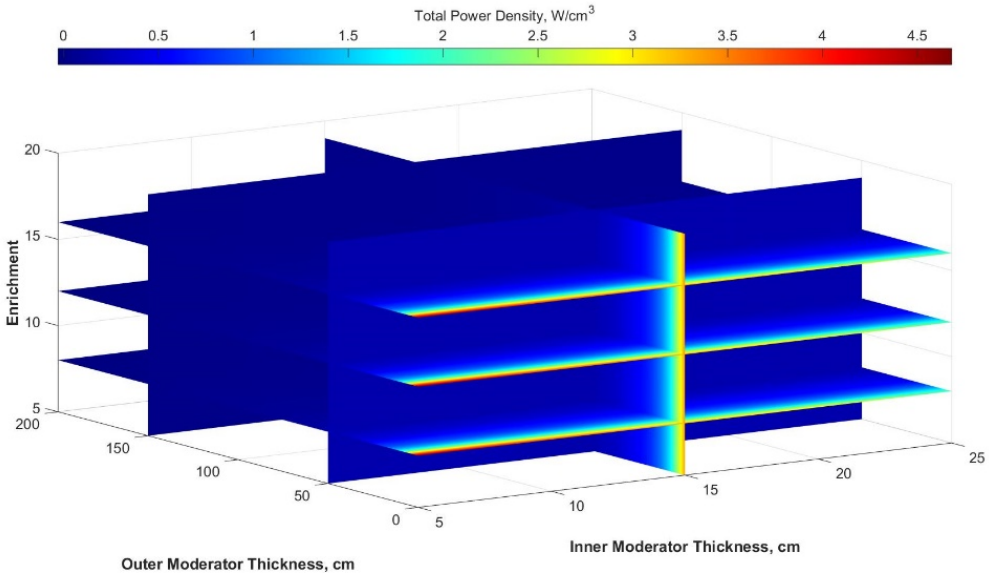

Figure 5.3. Power density as a function of enrichment, outer moderator thickness, and inner moderator thickness.

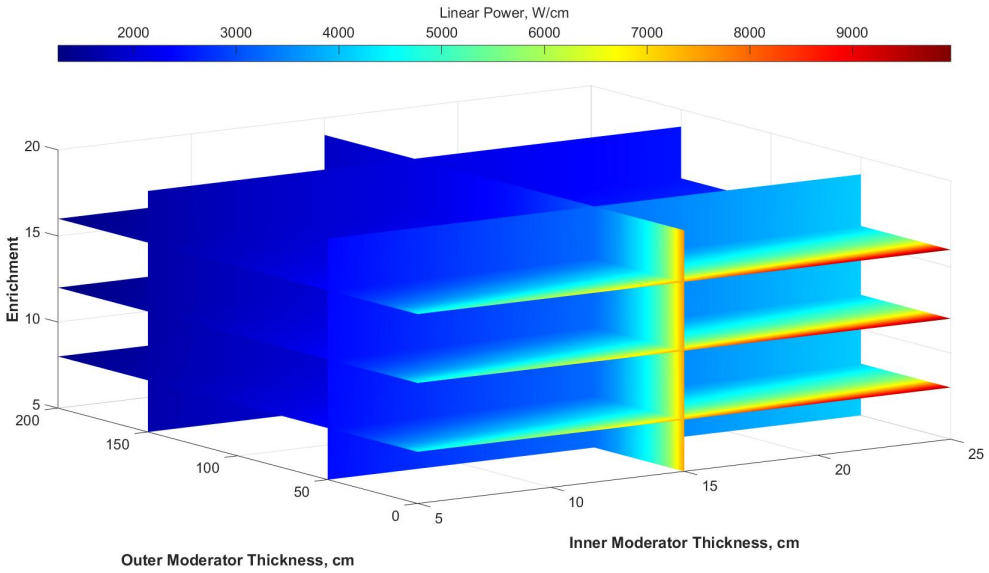

Figure 5.4. Total linear power as a function of enrichment, outer moderator thickness, and inner moderator thickness.

5.3 The Final Converged Design

The most favorable design with 19.75% enrichment and moderating ratio of 25 was selected from Table 5.1 as a significant improvement in terms of fuel utilization without too great

an addition to structural costs. The major design parameters for this case are given in Table 5.2. The parameters of this case were input into the top-down economic model to test the design's viability. A sensitivity study of these estimates, based on the newly selected point in the design space, was conducted, with results found in Appendix A.

Table 5.2. Design and operational parameters of the final converged design.

Parameter	Value
Inner Graphite Radius, cm	25
UN Fuel Radius, cm	34
Outer Graphite Radius, cm	128
Beryllium Reflector Radius, cm	129
Tungsten Emitter Radius, cm	129.5
Uranium Enrichment, %	19.75
Discharge Burnup, MWd/kgU	130
Power Density, W/cm^3	0.06

The best and average LCOE estimates, for a capitalized and annualized fuel plan, compared to data on reference electricity sources provided by the US EIA is presented in Figure 5.5 [45]. Again, the LCOE is broken into capital costs and fixed operating costs, variable operating costs in the form of fuel costs, and the USMR specific cost to replace the TPVs. This figure highlight two major factors about the economics. First, for this final converged case,the estimates show the USMR to produce electricity at comparable cost with current operating nuclear plants under average conditions and to provide electricity at half the cost under the best conditions. Secondly, for improved case, the breakdown of LCOE reveals that the fuel costs are a comparable portion of the total costs, but it also shows how the economic viability of the USMR project hinges on the cost of the initial core and replacing the TPVs.

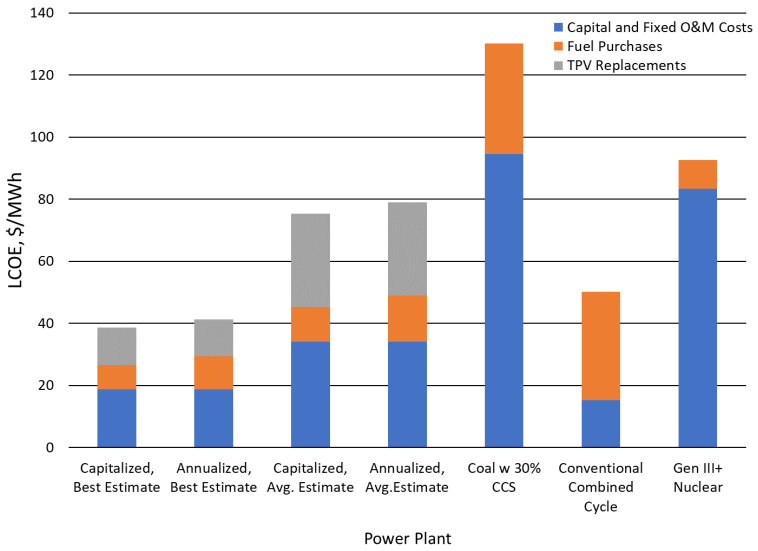

Figure 5.5. Comparison of the USMR Average and Best LCOE Estimates to different power sources and the breakdown of LCOE costs for USMR based on fuel purchase plan.

Lastly, the mapping, in the capital and operating cost space, of the four fuel purchasing plans using the favorable USMR design average and best estimates and reference electricity sources is shown in Figure 5.6. From this picture, it is clear to see that the favorable USMR design for the normal and ramped capitalized fuel plans fall in line with the standard baseload plants in the best conditions, but have significantly higher under the average estimates, which is entirely a factor of the TPV replacement costs. Under a multi-batch, annualized fuel plan, the favorable USMR design is competitive with typical mid-merit plants. The ability of the TPVs to rotate to instantaneously lower and raise electric output allows for the plant to actually fulfill the role of a load following plant. The typical nuclear plants are largely dependent on neutron kinematics to scale up and down electric output which limits the response time.

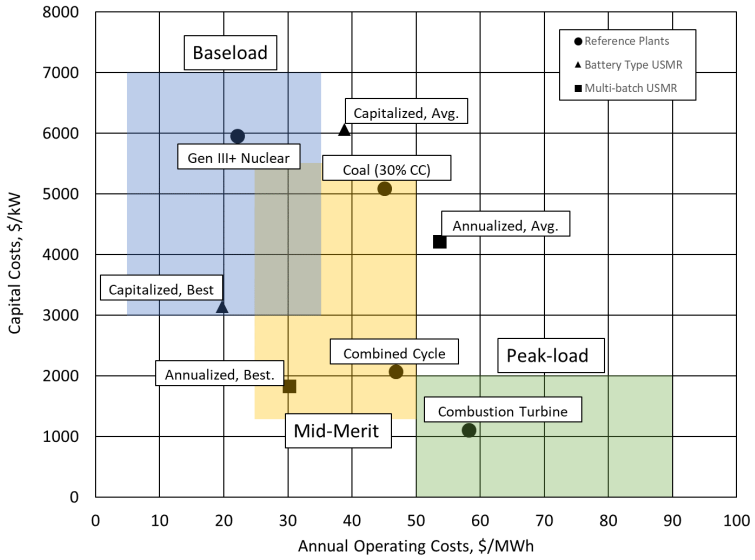

Figure 5.6. Comparison between the USMR best and average capital and operating cost estimates for various fuel purchasing plans and typical capital and operating cost of various power sources.

CHAPTER 6
FINAL REMARKS

6.1 Conclusion

This thesis has focused on the thorough development the USMR design from a pre-conceptual proposal to a full concept. After the shift to an economically driven design optimization, the USMR concept looks extremely promising, especially in light of the stochastic economic results and the high likelihood of developing an economic model. However,the development of the computational physics and economic modeling tools laid out previously have been the most significant part of this work, for those tools will be key in continuing to developing the USMR design.

Excluding the technical hurdles and validation studies that still need to be completed before implementation, there are many regulatory and practical road blocks to overcome. Some of these, the need to develop a reasonable licensing framework for plants built on multiple small and micro reactor units or the lack of production capacity for high assay, low enriched fuels, are already in the process of being resolved thanks to industry interest. Still, there are many USMR specific priorities including the licensing of uranium nitride fuels and the allowance for burnups that are twice the current limit. Overall, the pressing need for carbon free, distributed energy to combat climate change means that its imperative to rapidly push for the implementation of novel technologies such as the USMR.

6.2 Future Work

With the completion of the work presented in this thesis, the USMR project is ready to enter a new phase of development. The ongoing areas of work on the USMR can be divided into four categories: computational neutronic design, computational coupled analysis, bal-

ance of plant design, and experimental validation. First, under computational neutronics is the need development of explicit 3D models of the favorable design in order to design and study reactivity controls, axial multi-batch loading and axial reflectors. Second,for computational coupled analysis, there is the need to determine the material temperature reactivity coefficients for the USMR while hot and cold, to develop a transient tool to examine accident and operational variations, and to develop a 2D and 3D finite element codes for explicit final thermal analysis. Third, there is a need to determine the actual layout and siting of a USMR plant at a range of plants sizes as informed by the economics, shielding studies, and probabilistic risk assessment. Lastly, as mentioned, there is a lack of evidence on the functionality of TPVs within a reactor's radiation field which needs to be rectified. The purpose of much of this future work will be to validate many of the assumptions made in the development of the top-down differential economic model presented here.

Though the ongoing USMR project will be focused on developing a SMR that is competitive in near future energy markets, there is a potential secondary path for the basic USMR premise, one that is focused on the higher cost, but more compact design. Namely, this is the development of a safe, mobile nuclear generator that could be used for military, emergency response and space applications, both as a replacement for radiological thermoelectric generators and the deployment of nuclear electronic propulsion.

Appendices

APPENDIX A

ECONOMIC SENSITIVITY AT THE FINAL CONVERGED DESIGN

As part of a validation of the earlier economic sensitivity analysis, a second, parametric economic analysis was conducted starting from a default set of inputs, found in Table A.1, based around the final favorable design. Similar to the first sensitivity analysis, every variable in the table, was independently perturbed. The results of this study can be found in Figures A.1 to A.10, which show LCOE as a function of the given parameter being varied. As can be seen in the figures compared to those in Section 4.2.3, the same basic LCOE can be seen for each parameters. Also, once again the choice in fuel seems to have very little economic impact with uranium nitride being almost negligibly cheaper. However, the total costs are lower and the magnitude of some of the dependencies have changed.

Table A.1. Default design parameters from used in parametric analysis.

Parameter	Value
Plant Parameters	
Capacity Factor (%)	95
Energy (MW)	1000
Plant Efficiency (%)	60
Total Lifetime (yr)	60
Ramp Period (yr)	5
Construction Period (yr)	1
Fuel Purchasing Plan	Capitalized
Fuel Parameters	
Burnup (MWd/kgU)	130
Fuel Enrichment (%)	19.75
Total Power Density (W/cm3)	0.05
Fuel Material	UN

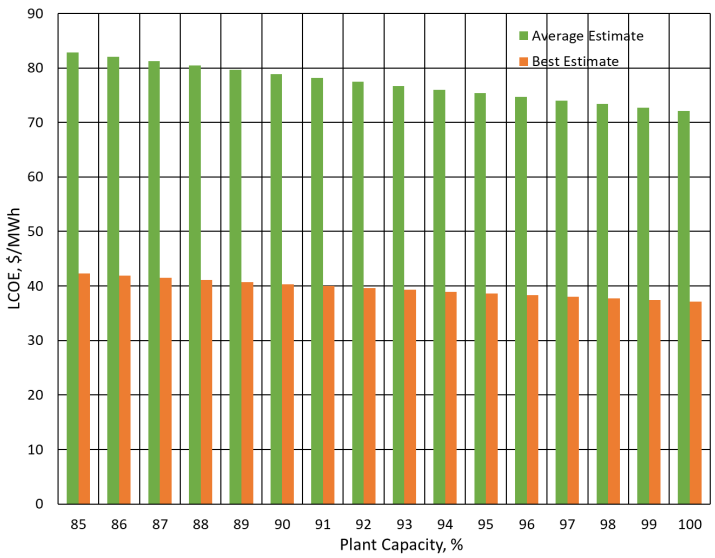

Figure A.1. LCOE estimates as a function of plant capacity.

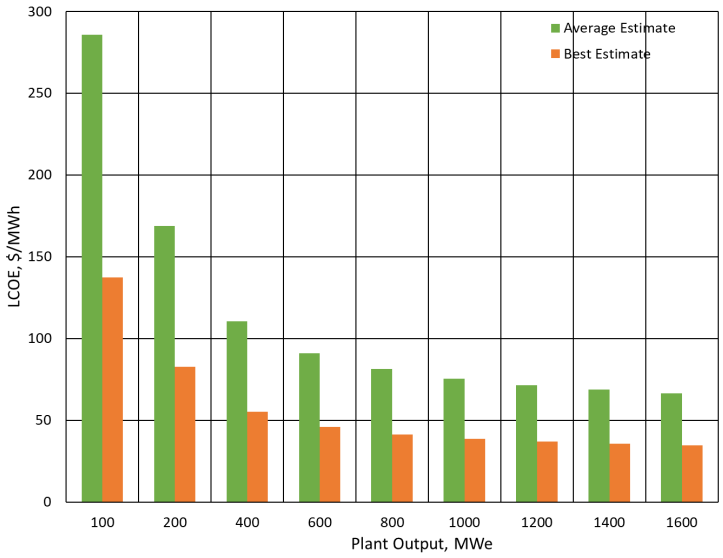

Figure A.2. LCOE estimates as a function of plant size.

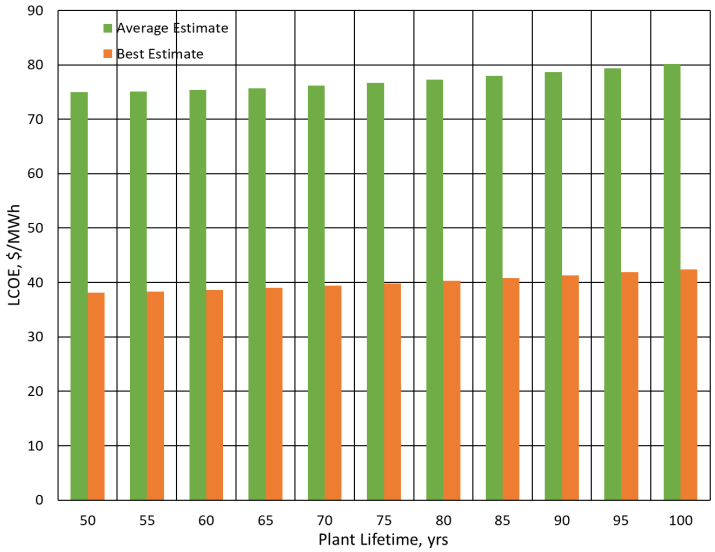

Figure A.3. LCOE estimates as a function of plant lifetime.

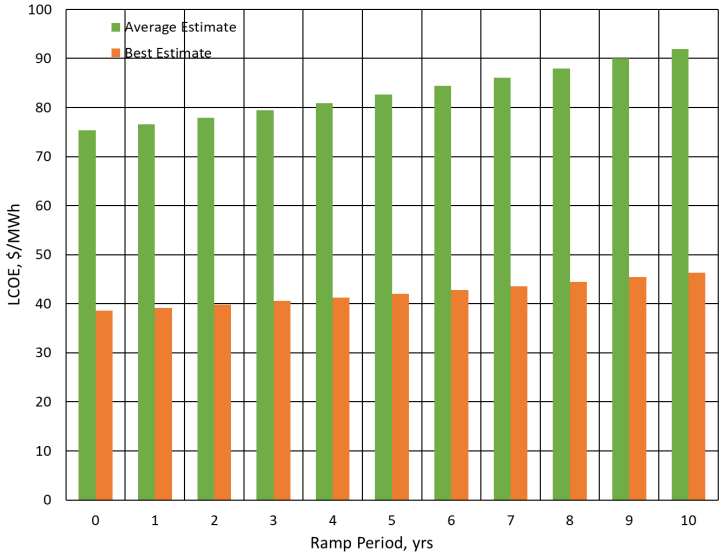

Figure A.4. LCOE estimates as a function of interval installation period.

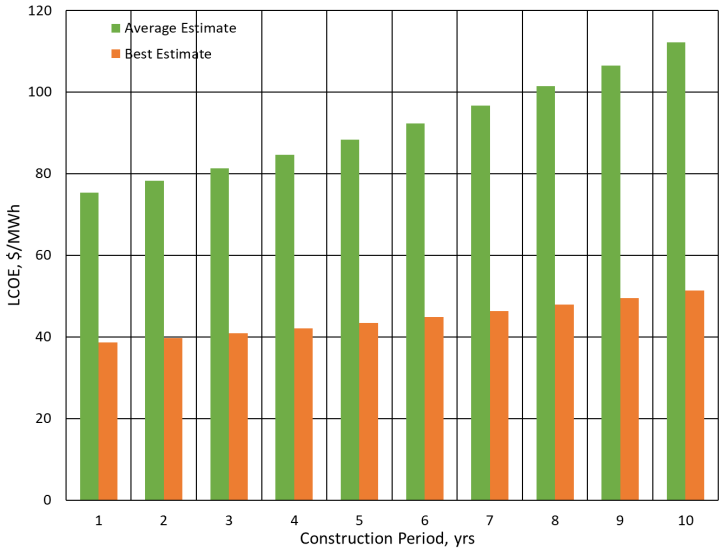

Figure A.5. LCOE estimates as a function of construction period.

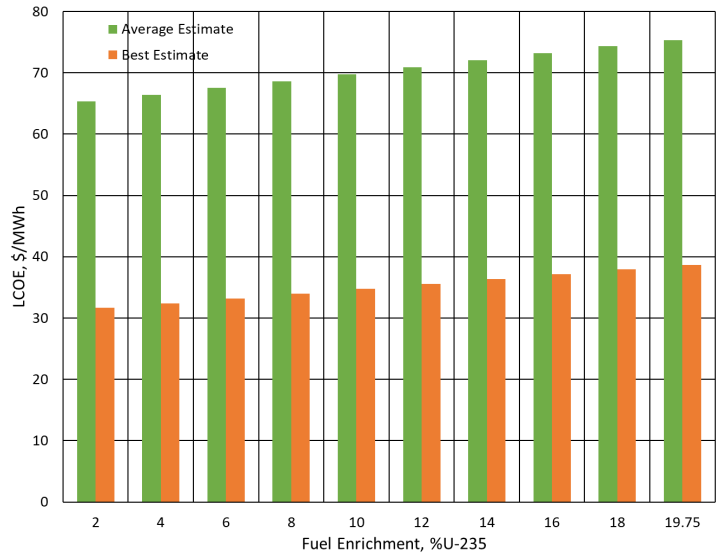

Figure A.6. LCOE estimates as a function of fuel enrichment.

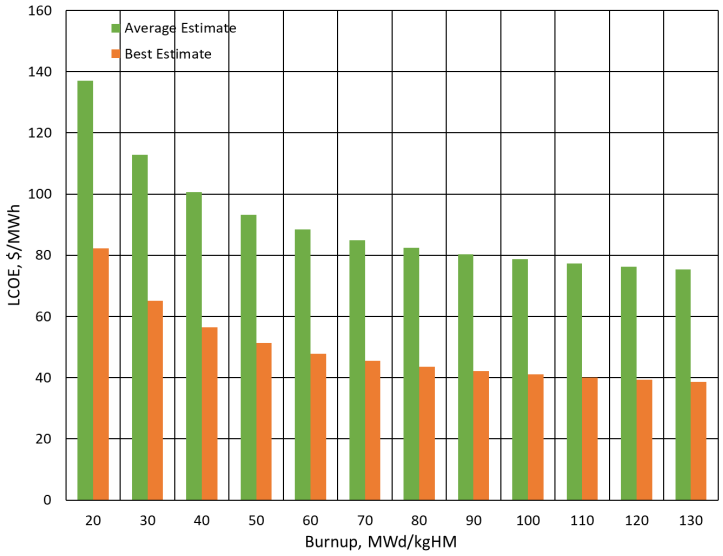

Figure A.7. LCOE estimates as a function of fuel utilization.

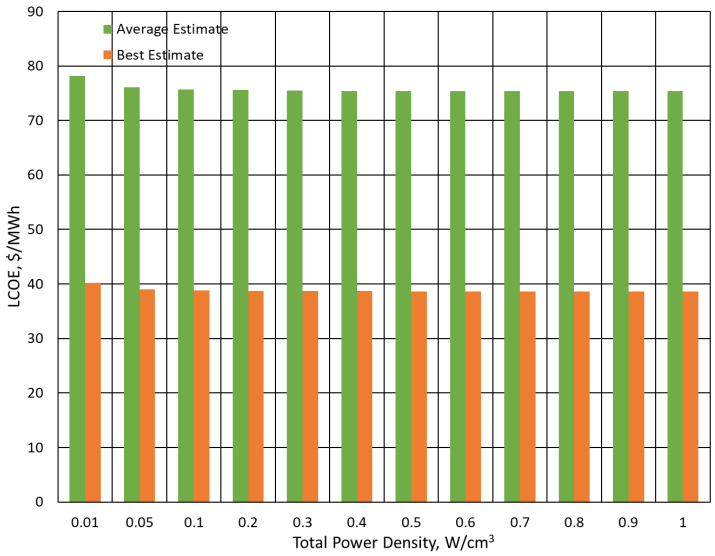

Figure A.8. LCOE estimates as a function of total power density of the core.

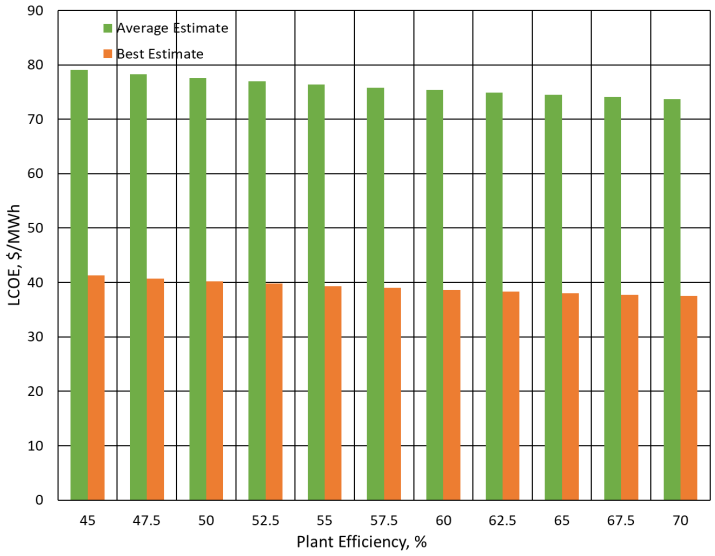

Figure A.9. LCOE estimates as a function of plant efficiency.

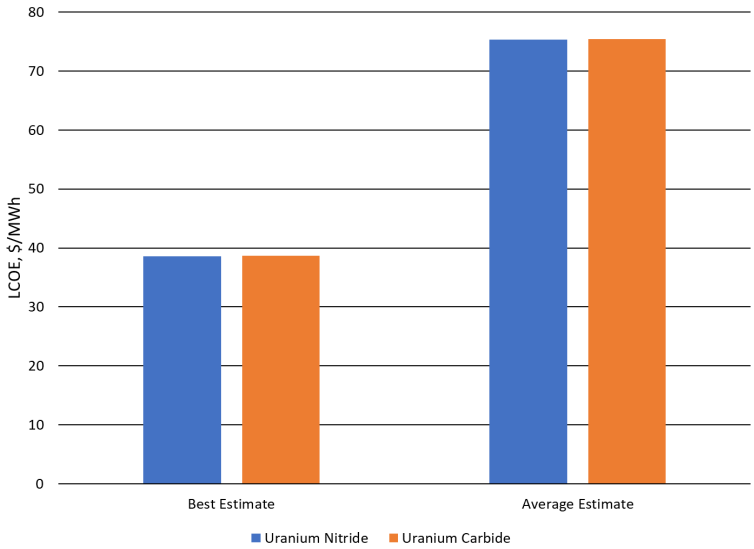

Figure A.10. Comparison of LCOE estimates for selection of uranium nitride and uranium carbide fuel.

The average relative differential, defined by the Equation A.1, was once again used to determine the magnitude of impact on LCOE and Capital Costs for each of the parameters and can be found in Table A.2. The majority of parameters are shown to have lower impact on the costs at this point in the design space. This is likely due to diminishing returns on design efforts to lower costs when starting from a much more economically favorable place. It is worth noting that in this point of the design space, burnup and capacity are now the most significant economic factors for the core and plant design parameters, in terms of LCOE. Notably, the least impactful factors have remained steady. Overall, the general recommendations from the first analysis are still applicable, which is what was desired.

$$\frac{dY/Y}{dX/X} \approx \Sigma \frac{1}{N} \frac{\frac{Y_{i+1}-Y_i}{Y_i}}{\frac{X_{i+1}-X_i}{X_i}} \tag{A.1}$$

Table A.2. The relative differential of the LCOE and capital costs based on changing design parameters.

Parameter	LCOE Relative Differential	Capital Costs Relative Differential
Plant Design Parameters		
Capacity	-0.846	0.300
Electricity Output	-0.303	-0.433
Construction Period	0.238	0.176
Plant Lifetime	0.103	0.345
Ramp Period	0.097	-0.036
Core Design Parameters		
Discharge Burnup	-0.230	-0.399
Plant Efficiency	-0.152	-0.309
Enrichment	0.080	0.176
Power Density	-0.002	-0.004

REFERENCES

[1] N. Kaffezakis, S. Terlizzi, C. Smith, A. Erickson, S. Yee, and D. Kotlyar, "High temperature ultra-small modular reactor: Pre-conceptual design," *Annals of Nuclear Energy*, 2019.

[2] T. Roulstone, "Nuclear at the crossroads," *Nuclear Future*, 2019.

[3] E. F. Mastal, "Phase viii update report for the energy economic data base program.," U.S. Department of Energy, Tech. Rep., 1986.

[4] "Technology roadmap for generation iv nuclear energy systems," Gen IV International Forum, Tech. Rep., 2002.

[5] S. Boarin and M. Ricotti, "An evaluation of smr economic attractiveness," *Science and Technology of Nuclear Installations*, 2014.

[6] "Technical and economic aspects of load following with nuclear power plants," Nuclear Energy Agency, Tech. Rep., 2011.

[7] "Technology roadmap update for generation iv nuclear energy systems," Gen IV International Forum, Tech. Rep., 2014.

[8] H. R. Seyf and A. Henry, "Thermophotovoltaics: A potential pathway to high efficiency concentrated solar power," *Energy and Environmental Science*, vol. 9, pp. 2654–2665, 2016.

[9] R. L. Crabb, "Solar cell radiation damage," *Radiation Physics*, vol. 43, 1994.

[10] V. Arora, "Levelized cost and levelized avoided cost of new generation resources in the annual energy outlook 2018," U.S. Energy Information Agency, Tech. Rep., 2018.

[11] P Clerens, M Farley, L Jazbec, N Kraus, and K. Tigges, "Thermal power in 2030 added value for eu energy policy," *European Power Plant Suppliers Association*, 2015.

[12] "Nuclear reactor, state, and net capacity," U.S. Energy Information Administration, Tech. Rep., 2018.

[13] M. Carelli, B. Petrovic, and C. W. Mycoff, "Economic comparison of dfferent size nuclear reactors," *Proceedings IJM Cancun 2007*, pp. 653–662, 2007.

[14] S. Patel, "How the vogtle nuclear expansion's costs escalated," *Power*, 2018.

[15] "Monthly electric generator inventory based on form eia-60," U.S. Energy Information Administration, Tech. Rep., 2019.

[16] J. Holman, *Heat Transfer*. McGraw-Hill Book Company, 1986.

[17] A. Webb J and I. Charit, "Analytical determination of thermal conductivity of w–uo2 and w–un cermet nuclear fuels," *Journal of Nuclear Materials*, vol. 427, 87–94, 2012.

[18] S. Hayes, "Material property correlations for uranium mononitride. iv. thermodynamic properties.," *Journal of Nuclear Materials*, vol. 171, 300–318, 1990.

[19] J. Lewis, "Estimating thermal conductivity of cermet fuel materials for nuclear reactor application," Lewis Research Center, Cleveland, Ohio, Tech. Rep. Tech. Rep. NASA TN D-3898, 1967.

[20] B. Panda, R. R. Hickman, and S. Shah, "Solid solution carbides are the key fuels for future nuclear thermal propulsion," in *Joint Army-Navy-NASA-Air Force (JANNAF);*, American Nuclear Society, Monterey, CA; United States, 2005.

[21] L. L. Lyon, "Performance of (u, zr)c-graphite (composite) and of (u,zr)c (carbide) fuel elements in the nuclear furnace 1 test reactor," Los Alamos National Laboratory, Los Alamos, New Mexico, Tech. Rep. LA-5398-MS, 1973.

[22] P. Avigni, "On-line refueling for the advanced high temperature reactor," PhD thesis, Georgia Institute of Technology, 2017.

[23] J. Gates, A. Denig, R. Ahmed, M. V.K., and K. D., "Low-enriched cermet-based fuel options for a nuclear thermal propulsion engine," *Nuclear Engineering and Design*, vol. 331, pp. 313 –330, 2018.

[24] J. Leppänen and e. al., "The serpent monte carlo code: Status, development and applications in 2013," *Annals of Nuclear Energy*, vol. 82, pp. 142–150, 2015.

[25] G. Maronati, B. Petrović, and N. Čavlina, "I2s-lwr top-down differential economics evaluation approach," *Energija*, vol. 65, no. 1-2, pp. 0–0, 2016.

[26] W. e. a. Rasin, "Cost estimating guidelines for generation iv nuclear energy seystems.," Generation IV International Forum, Tech. Rep., 1986.

[27] J. McDaniel, T. Dorn, and S. Shimmin, "Land values 2017 summary," United States Department of Agriculture, Tech. Rep. 1949-1867, 2017.

[28] B. Edge, "Commission approves agreement on georgia power integrated resource plan; increases renewable energy resources; approves capitalization of costs for early development of stewart county nuclear power facility," Georgia Public Service Commission, Tech. Rep., 2016.

[29] "Westinghouse technology manual," Nuclear Regulatory Commission, Tech. Rep. ML023040268, 2002.

[30] H. Bowers, L. Fuller, and M. Myers, "Cost estimating relationships for nuclear power plant operations and maintenance," Oak Ridge National Lab., TN (USA), Tech. Rep., 1987.

[31] D. Mase, "How to build an employee relocation package," *Urban Bound*, 2018.

[32] K. Pomerleau, "A comparison of the tax burden on labor in the oecd, 2014," 2014.

[33] N. E. AGENCY, "Decommissioning nuclear power plants: Policies, strategies and costs," ORGANISATION FOR ECONOMIC CO-OPERATION and DEVELOPMENT, Tech. Rep., 2003.

[34] Metal. (2019). Beryllium.

[35] Metalary. (2019). Tungsten price.

[36] Power and U. O. Team, "2017 uranium marketing annual report," U.S. Energy Information Administration, Tech. Rep., 2018.

[37] F. Gao and W. I. Ko, "Dynamic analysis of a pyroprocessing coupled sfr fuel recycling," *Science and Technology of Nuclear Installations*, vol. 2012, 2012.

[38] B. Bonner, "Current hydrogen costs," DOE Hydrogen and Fuel Cell Technical Advisory Committee, Tech. Rep., 2013.

[39] G. Elert, "The physics hypertextbook," 2019.

[40] B. G., "Northern graphite corporation a pre-development stage graphite company," Northern Graphite Corporation, 2019.

[41] "Uranium enrichment," World Nuclear Association, Tech. Rep., 2019.

[42] A. Van Heek, F. Roelofs, and A. Ehlert, "Cost estimation with g4-econs for generation iv reactor designs," in *GIF Symposium Proceedings*, Generation IV International Forum, San Diego, CA; United States, 2012.

[43] NRC, "Revision of fee schedules; fee recovery for fiscal year 2018," Federal Register, Tech. Rep. 83 FR 29622.

[44] A. McDonald and L. Schrattenholzer, "Learning rates for energy technologies," *Energy policy*, vol. 29, no. 4, pp. 255–261, 2001.

[45] C. Namovicz and J. Diefenderfer, "Capital cost estimates for utility scale electricity generating plants," U.S. Energy Information Agency, Tech. Rep., 2016.